An Engineering Evaluation of Acoustic Methods of Leak Detection in Aboveground Storage Tanks

HEALTH AND ENVIRONMENTAL AFFAIRS
API PUBLICATION NUMBER 322
JANUARY 1994

Strategies for Today's Environmental Partnership

American Petroleum Institute
1220 L Street, Northwest
Washington, D.C. 20005

An Engineering Evaluation of Acoustic Methods of Leak Detection in Aboveground Storage Tanks

Health and Environmental Affairs Department

API PUBLICATION NUMBER 322

PREPARED UNDER CONTRACT BY:

JAMES W. STARR, AND JOSEPH W. MARESCA, JR.
VISTA RESEARCH, INC.
MOUNTAIN VIEW, CALIFORNIA

AUGUST 1993

American
Petroleum
Institute

FOREWORD

API PUBLICATIONS NECESSARILY ADDRESS PROBLEMS OF A GENERAL NATURE. WITH RESPECT TO PARTICULAR CIRCUMSTANCES, LOCAL, STATE, AND FEDERAL LAWS AND REGULATIONS SHOULD BE REVIEWED.

API IS NOT UNDERTAKING TO MEET THE DUTIES OF EMPLOYERS, MANUFACTURERS, OR SUPPLIERS TO WARN AND PROPERLY TRAIN AND EQUIP THEIR EMPLOYEES, AND OTHERS EXPOSED, CONCERNING HEALTH AND SAFETY RISKS AND PRECAUTIONS, NOR UNDERTAKING THEIR OBLIGATIONS UNDER LOCAL, STATE, OR FEDERAL LAWS.

NOTHING CONTAINED IN ANY API PUBLICATION IS TO BE CONSTRUED AS GRANTING ANY RIGHT, BY IMPLICATION OR OTHERWISE, FOR THE MANUFACTURE, SALE, OR USE OF ANY METHOD, APPARATUS, OR PRODUCT COVERED BY LETTERS PATENT. NEITHER SHOULD ANYTHING CONTAINED IN THE PUBLICATION BE CONSTRUED AS INSURING ANYONE AGAINST LIABILITY FOR INFRINGEMENT OF LETTERS PATENT.

ABSTRACT

The design of an aboveground storage tank (AST) leak detection system based upon passive-acoustic methods requires a detailed understanding of the acoustic leak signal and the ambient noise field against which the signal is measured. As part of Phase III of the American Petroleum Institute's (API's) project to develop and evaluate the performance of different technologies for detecting leaks in the floor of ASTs, a set of controlled experiments was conducted in a 40-ft-diameter tank during June 1992. Two sets of holes of various diameters, ranging from 0.5 to 3 mm, were drilled in the tank floor. These holes released product (water) into one of two backfill materials: native soil or sand. Two types of acoustic signals were generated and studied: (1) the continuous leak signal produced by turbulent flow through a hole in the floor of the tank, and (2) the impulsive leak signal produced by bubbles collapsing in the backfill beneath the tank floor.

The analytical and experimental results of this project suggest that a passive acoustic system can be used to detect small leaks in ASTs. The experiments have shown that the impulsive leak signals identified through laboratory and field simulations are persistent and measurable within an AST. The experiments yielded two very significant findings, which must be addressed in the data collection and signal processing schemes used to detect leaks with the passive-acoustic method: (1) the multipath signals (leak-to-wall-to-sensor or leak-to-surface-to-sensor), which are associated with the direct path signal (leak-to-sensor), are very strong and may be stronger than the direct path signal, and (2) the time delays of the multipath signals relative to the direct path signal for each sensor in the wall array may be very different. Both phenomena are due to acoustic propagation in the highly reflective confines of a right circular cylinder AST.

During the experiments, a data collection procedure and a signal processing algorithm were used to separate the impulsive events associated with the leak from the strong multipath reflected signals. All of the leaks that were generated in the floor of the 40-ft-diameter tank were successfully detected and located.

ACKNOWLEDGMENTS

We wish to express our gratitude to the members of the API Storage Tank Task Force and the Work Group for AST Monitoring for their cooperation, their technical support, and their assistance in coordinating this project. We would like to acknowledge the support and encouragement of the chairperson of the Work Group, Mr. James Seebold, and the API staff member monitoring the program, Ms. Dee Gavora. We especially acknowledge the help of Mr. John Collins, of Mobil Oil, who provided technical input to the research and was instrumental in coordinating the field tests at the Mobil Refinery in Beaumont, Texas. For their helpful suggestions in reviewing this document, we would like to acknowledge Det Norske Veritas, Inc., CTI, Inc., and Physical Acoustics Corporation. Finally, we acknowledge the help of Monique Seibel and Christine Lawson of Vista Research in editing and typesetting this document.

TABLE OF CONTENTS

EXECUTIVE SUMMARY

INTRODUCTION

The design of a leak detection system based upon passive-acoustic methods requires a detailed understanding of the acoustic leak signal and the ambient noise field against which the signal is measured so that robust data collection and signal processing algorithms can be developed. As part of Phase III of the American Petroleum Institute's (API's) project to enhance and evaluate the performance, in actual operational environments, of different technologies for detecting leaks in the floor of aboveground storage tanks (ASTs), a set of controlled experiments was conducted in a 40-ft-diameter tank at the Mobil Oil refinery in Beaumont, Texas, during June 1992.[1] The tank was filled with water and two sets of holes of different diameters, ranging from 0.5 to 3 mm, were drilled in its floor. The holes in the center of the tank floor released product into a native-soil backfill, and the holes along the periphery of the tank floor released product into a sand backfill. Two types of acoustic leak signals were generated and studied under realistic conditions: (1) the continuous leak signal produced by turbulent flow through a hole in the floor of the tank and (2) the impulsive leak signal produced by bubbles collapsing in the backfill beneath the tank floor.

BACKGROUND

The API has completed three phases of a leak detection project for ASTs. The purpose of Phase I was to assess different leak detection technologies to determine which had the greatest potential for field application. Phase II addressed in detail two of the methods studied in Phase I: passive-acoustic and volumetric methods. Phase III built on the insight gained in Phase II with regard to the acoustic leak signal and ambient noise field.

The objectives of Phase III, which addressed both volumetric and passive-acoustic leak detection technologies, were:

- to determine, in the case of acoustic methods, the nature of the acoustic leak signal resulting from realistic leaks in the floor of an operational AST;
- to determine, in the case of volumetric systems, if differential pressure (mass-measurement) systems have significant advantages over the conventional level and temperature measurement systems;

1 Experiments were also conducted as part of Phase III to evaluate the performance of volumetric methods of leak detection for ASTs. The results of the volumetric study are provided in a separate API document entitled *An Engineering Evaluation of Volumetric Methods of Leak Detection Systems for Aboveground Storage Tanks* by James W. Starr and Joseph W. Maresca, Jr.

- to characterize the ambient noise encountered under a wide range of test conditions for both detection technologies;
- to evaluate data collection and signal processing techniques that would allow the detection of the leak signal against the ambient noise;
- to identify any operational issues for implementation of methods based on either technology;
- to demonstrate the capabilities and, if possible, make an estimate of the performance, of both technologies through field tests; and
- to identify, in the case of both volumetric and passive-acoustic technologies, those features of a leak detection test that are necessary for achieving high performance.

CONCLUSIONS

The analytical and experimental results of this project suggest that a passive-acoustic system can be used to detect small leaks in ASTs. The experiments have shown that the impulsive leak signals identified through laboratory and field simulations during Phases II and III appear to be persistent and are measurable within an AST.

The experiments yielded two very significant findings, which *must* be addressed in the data collection and signal processing schemes used to detect leaks with passive-acoustic methods: (1) the multipath signals (leak-to-wall-to-sensor or leak-to-surface-to sensor), which are associated with the direct-path signal (leak-to-sensor), are very strong and may often be stronger than the direct-path signal, and (2) the time delays of the multipath signals relative to the direct-path signal for each sensor in the wall array may be very different.

Both phenomena are due to acoustic propagation in the highly reflective confines of a right circular cylinder AST. The former phenomenon, which is produced by wall focusing, is particularly important, because the inherent assumption in the design of the existing acoustic detection algorithms is that the largest leak signal is produced by the direct-path signal. The impulsive leak signal is detectable, because, as part of the signal processing, the direct-path signal can be distinguished in time delay from the multipath signals associated with it. While the multipath complicates the signal processing for impulsive leak signals, it makes it impractical to exploit the persistent leak signal.

During the experiments, a data collection procedure and a signal processing algorithm were used to separate the impulsive events associated with the leak from the strong multipath reflected signals. All of the leaks that were generated in the floor of the 40-ft-diameter tank were successfully detected and located.

This document presents the results of these acoustic experiments in two separate technical papers, which are attached as appendices. The first discusses the characteristics of the acoustic leak signal and ambient noise field in an AST, and the second presents an engineering assessment of a methodology for detecting small leaks in the tank floor.

1 INTRODUCTION

This report summarizes Phase III of a research program conducted by the American Petroleum Institute (API) to evaluate the performance of different technologies that can be used to detect leaks in the floors of aboveground storage tanks (ASTs). During Phase I, an analytical assessment of the performance of four leak detection technologies was investigated (Vista Research, Inc., 1989; Maresca and Starr, 1990). The four technologies included: (1) passive-acoustic sensing systems, (2) volumetric systems, especially differential pressure (or ''mass'') measurement systems, (3) enhanced inventory reconciliation methods, and (4) tracer methods. During Phase II, field tests were conducted on a 114-ft-diameter AST containing a heavy naphtha. The purpose of these tests was to make an engineering assessment of the performance of two of the above technologies, passive-acoustic sensing systems and volumetric detection systems. These tests were conducted at the Mobil Oil Corporation refinery in Beaumont, Texas, during May 1992. The results of the Phase II research program are described in two API final reports and three professional papers (Vista Research, Inc., 1991, 1992; Eckert and Maresca, 1991, 1992). During Phase III, additional field tests were conducted on a pair of ASTs in order to test the acoustic and volumetric leak detection strategies that emerged from the Phase II study and to further evaluate the current state of leak detection technology. These tests were also conducted at the Mobil refinery at about the same time of year as the Phase II tests. The acoustic tests were conducted in a 40-ft-diameter AST containing water, and the volumetric tests in a 117-ft-diameter tank containing a light fuel oil. In the case of the acoustic tests, holes were drilled in the floor of the tank to allow realistic simulation of leaks into two different types of backfills beneath the floor. This report describes the results of the Phase III acoustic tests; the results of the volumetric tests are described in a separate report, which consists of a brief overview of the work and two technical papers (Vista Research, Inc., 1993).

The specific objectives of the Phase III acoustic experiments were:

- to characterize the two general types of acoustic leak signals (i.e., continuous and impulsive) produced by leaks in the floor of an operational AST;
- to characterize the ambient noise that would interfere with each type of acoustic leak signal and that would be found in a typical AST under a wide range of refinery and environmental conditions;
- to demonstrate in a series of field tests data collection and signal processing techniques that would allow the detection of leaks in the floor of an AST; and

- to identify those features of a leak detection test that are crucial to achieving high performance.

The body of this report consists of a short technical summary of the work. Section 2 summarizes the relevant Phase II results that were further investigated in Phase III. Sections 3 and 4 summarize the important results, conclusions, and recommendations of this experimental project. Section 5 presents the general features of a passive-acoustic method that will achieve a high level of performance. A detailed description of the field tests and analyses are presented in two professional papers, which are attached as appendices to the report.

2 BACKGROUND

The choice of a particular strategy for the acquisition and processing of acoustic signals is strongly tied to the nature of the signal and the background noise field in which the signal is immersed. Studies of simulated leak signals have shown that the acoustic signal produced by a leak contains two distinctly different components (Vista Research, Inc., 1992; Eckert and Maresca, 1991, 1992). Turbulence associated with the leak flow field produces a *persistent* acoustic signal that is believed to be present in all AST leaks. The magnitude of the persistent leak signal is dependent upon the backfill conditions beneath the AST floor and on the flow rate through the hole in the floor. The second type of acoustic leak signal is *impulsive* in character and is caused by the interaction of air bubbles beneath the AST with the turbulent leak flow field. While the impulsive leak signal is much greater in magnitude than the persistent signal, the degree to which the impulsive signal is associated with AST leaks is unknown. Phase II laboratory tests showed that air must be entrained into the leak flow field in order for an impulsive signal to be produced; no impulsive signals were observed when the backfill was completely saturated with product or groundwater. The approach to AST acoustic leak detection adopted by the industry exploits only the impulsive component of the leak signal. This approach is based upon the success with which flaws and cracks in a variety of materials have been identified through the use of acoustic emissions (AE) techniques. Though a number of firms offer AST leak detection services based upon passive acoustics, very little technical information has been published concerning the performance of such systems or the nature of the acoustic signal produced by leaks in operational ASTs. Many proven techniques have been developed in order to locate sources of continuous signals, for example, sonar and radar beamforming systems. The primary focus of the API work is the development of data acquisition and signal processing techniques that will allow the impulsive and/or the persistent components of the acoustic leak signal to be successfully exploited for the purpose of leak detection.

The Phase III field tests were designed to evaluate and refine the results of the Phase II tests. The most important results of the Phase II experiments and analyses are summarized below.

- Many of the false alarm and missed detection problems experienced by commercial vendors are predictable and can be attributed to inadequate data collection and signal processing algorithms; they are produced by the use of a detection threshold that is too low compared to background noise, by improper time registration of signal events, and by incorrect assumptions that large noise events are signal events. The typical threshold settings used by the testing community are based upon the persistent contributions to the ambient noise field, which leads to an excessive number of threshold exceedances based solely on the noise and not the leak signal or the impulsive noise that might mask the leak signal. Observations of the leak signal suggest it is 10 to 20 times larger than the persistent noise. To process the data, the acoustic signal from each individual collapsing bubble event must be correctly identified by each acoustic sensor. If acoustic signals from different bubble events are processed together, then erroneous location estimates are made. This mixing of the impulsive leak signals is difficult to avoid unless a continuous time history of data is collected. Because none of the vendors is recording continuous time histories, impulse mixing cannot be avoided with the AE data collection approach, and it becomes an important source of error. Simple calculations, assuming only the presence of leak signals (i.e., no noise), suggest that the probability of a false alarm is 50% if the rate of occurrence of events is 12 per second. The probability of false alarm increases dramatically if the rate of occurrence is higher or if the ambient noise is also included in the calculation. These problems can be minimized by collecting data continuously, using a higher threshold for detection, devising better sensor geometry, and employing more robust algorithms to identify and avoid noise. A detailed description and analysis of these problems are provided by Eckert and Maresca (Vista Research, Inc., 1992; Eckert and Maresca, 1991).

- The strongest acoustic signal produced by a hole in the floor of a tank propagates through the liquid. Sensors responded similarly to the impulsive leak signal regardless of whether they were submerged in the liquid inside the tank or located on the exterior wall of the tank. The noise field seemed to be lower, however, for the submerged sensors than for those mounted on the wall. The multipath reflections observed in the data are predictable using simple ray tracing techniques.

- Both the persistent and impulsive signals exhibited a positive signal-to-noise ratio. More information is required about the characteristics of the persistent signal, however, before a determination can be made on whether such a signal can be successfully exploited. More information is also required about the impulsive signal so that more robust data collection and signal processing algorithms can be developed.

- The only mechanism that produced strong impulsive signals in the laboratory tests was the collapsing of air bubbles in the flow field of a well-drained backfill beneath the tank. When the backfill became saturated and all the entrained air escaped, the impulsive signal ceased. This raised questions about whether such a signal would persist in an operational environment where the void space that develops in the backfill beneath the leak could fill with product (or with water resulting from precipitation that accumulates in the diked areas surrounding the AST). Except for the Phase II laboratory experiments, the controlled experiments that were used by the commercial testing community to develop their testing approach were conducted under extremely well-drained backfill conditions in which such a signal would always be present. More realistic information about the presence and persistence of the impulsive acoustic leak signal is needed in order to justify the exploitation of this signal.

- A signal-processing approach that uses a beamforming algorithm was developed as a means to exploit both the persistent and impulsive leak signals. Exploitation of the persistent signal is the primary reason for using this approach. The beamforming approach requires a high degree of similarity between the signal wave forms recorded by spatially separated sensors. Stated another way, the coherence between any two time series containing the signal should be high in the signal frequency band. If the coherence of the persistent leak signal is found to be high between the various sensors in the wall-mounted arrays, the performance achieved using this signal should be as good as, if not better than, the conventional leading-edge, threshold-detection approach being used by industry for impulsive signals. The performance of the beamforming approach increases as the number of sensors and the integration time increase.

- The optimal configuration for acoustic sensors in an AST should incorporate the following: (1) an array of sensors that are separated both vertically and horizontally so that surface noise and reflected signals can be distinguished from leak signals emanating from the bottom; (2) one or more subarrays of closely spaced sensors for time registration; and (3) one or more subarrays of widely spaced sensors for accuracy in locating the leak. Optimal geometries for radar and sonar sensors consist of one wide-aperture array that has three narrow-aperture subarrays and that provides for both horizontal and vertical separation of sensors. Theoretically this would be an ideal configuration for acoustic sensors in an AST. However, the beam pattern resulting from a point response must be calculated before any sensor geometry can be finalized.

3 SUMMARY OF RESULTS

Three types of field experiments were performed in Phase III. The first type was designed to characterize the acoustic signal produced by a hole in the tank, the second to characterize the ambient noise field that existed during the entire data collection period, and the third to assess the merits of the data collection and signal processing approach developed in Phase II. Two sets of tests (each including all three types of experiments) were conducted, one to exploit the persistent leak signal and one to exploit the impulsive leak signal.

All of the acoustic experiments in this phase of the API project were conducted in a 40-ft-diameter AST especially outfitted with controllable leaks for these tests. The tank was filled with water to a depth of 25 ft for all of the tests. Three sets of holes were used to investigate the nature of the acoustic leak signal. Five holes ranging in diameter from 0.5 to 3 mm and spaced at 5-ft intervals were drilled into the floor near the center of the tank; a similar set of holes was drilled near the tank walls. The backfill under the center holes was native soil, and that under the side holes was sand. A leak simulator having a similar configuration was also installed in the tank, but at a different location; in the simulator, the flow rate of the leak could be controlled and measured. A specially designed flowmeter was used to measure the flow rate in each floor hole. A hydrophone was used to verify that each hole not used to generate a leak during a test was closed and did not generate any additional acoustic leak signals. The smallest hole in the AST that produced a measurable flow rate was 2.0 mm in diameter. The three holes smaller than 2.0 mm were presumed to be clogged with debris. The lack of flow in these smaller holes was verified with the flowmeter and a hydrophone.

The AST had a false bottom that was filled with sand. A section of the false bottom was removed for these tests, and the sand under this section was replaced with the native-soil backfill. Large-amplitude, impulsive leak signals were observed whether the leak flowed through the false bottom into a sand backfill or through the "single bottom" into a native-soil backfill. However, both the frequency and strength of the impulsive leak signals were dependent upon the backfill material and backfill conditions. The leak from the 2.0-mm-diameter hole in the false bottom into the sand backfill produced impulses at a greater rate (typically 1 to 20 per minute) than did the corresponding leak from the single bottom into native soil (typically 1 every 5 minutes). The frequency of these signals was significantly lower than that of the impulsive signals measured in the laboratory (typically 10 to 50 per second) in well-drained, granular backfills. The broadband frequency content of the impulsive leak signal, combined with the low level of ambient noise observed at frequencies above 10 kHz, allowed the impulsive signal to be easily detected by both internal and external sensors. The impulsive leak signal was generally 10 to 20 times larger than the standard deviation of the random ambient background noise.

The persistent leak signal associated with turbulent flow and the entrainment of small-diameter particulates into the leak flow field was detectable above the ambient noise. However, at frequencies below 10 kHz, the leak signal was largely masked by ambient noise. Persistent leak signals produced by the 2.0-mm-diameter leak through the false bottom into the sand were significantly larger in amplitude than those produced by the corresponding leak through the single bottom into native soil. If the time history of the no-leak condition were not available for comparison, however, one would have no way to determine, based on signal strength alone, if the acoustic data were produced by noise or a leak signal.

Measurements of the acoustic leak signal are made against a noise field that is highly variable both in strength and frequency distribution. The complex variety of noise sources encountered at a refinery ensures that acoustic data recorded within any frequency band and over any time scale are subject to some form of contamination by ambient noise. Sources of persistent acoustic noise observed during the field tests included industrial activities associated with the refinery and nearby factories, traffic, and leaking valves in aboveground steam-distribution pipelines. While these sources produce consistently high levels of ambient noise, the frequency content of persistent noise is largely confined below 10 kHz. Distinctive, impulsive sources of noise are also observed as part of the AST ambient noise environment. Mechanisms observed to cause impulsive noise included rain, condensation, and mechanical stresses imparted to the AST through connecting pipelines during product transfers. Most impulsive noise sources can be effectively avoided through careful choice of the measurement period and sensor location or minimized through robust data collection and signal processing.

The current method by which the presence of an AST leak is inferred is detection-through-location. This approach requires that the differential arrival time of acoustic signals at the elements of a sensor array be measured. Accurate source location (and hence acceptable performance as a leak detection system) demands that the recorded signals maintain a high degree of similarity with respect to one another. The similarity between time series of both impulsive and persistent leak signals recorded by spatially separated sensors was degraded by multipath signal propagation within the reflective confines of the AST. The observed lack of coherence between measurements of the persistent leak signal was such that the differential arrival time of the signal could not be measured. The low coherence, which was observed at sensor separations of only 4 in., is due to multipath reflections resulting from the circular geometry of the tank. As a consequence, the persistent leak signal cannot be exploited for the purpose of leak detection and instead must be viewed as a source of noise.

Investigations of multipath propagation within the AST were conducted through measurements of the impulsive leak signal and through ray-tracing simulations. The ray-tracing simulations, which modeled single and double reflections of impulsive signals from the AST shell and air-/water interface, accounted for much of the observed multipath contamination of impulsive leak signals. Experimental evidence that the amplitude of multipath signals could actually exceed that of the direct-path (source-to-sensor) signal was supported by the results of the ray-tracing studies. That the direct path acoustic return may not be the strongest signal has significant ramifications in the design of a robust leak detection system since all the detection algorithms assume that the direct-path impulsive signal is stronger than the multipath reflections. A simulation was conducted which showed that a wide-aperture array of externally mounted sensors will be subject to multipath contamination regardless of the location of the leak.

Leak detection experiments that concentrated on the impulsive component of the leak signal were conducted using a pair of 2.0-mm-diameter leaks and the leak simulator. Because the impulsive signals appear infrequently, data acquisition was initiated by the exceedance of a preset threshold signal level at one element of a sensor array. The collected data consisted of continuous time series of the leak signal that contained the impulsive event. Although multipath propagation reduces the similarity between time series of impulsive leak signals, successful detection of leaks based upon these signals was accomplished through the application of a data quality test to each set of time series and the processing of these time series by a modified beamforming algorithm. The data quality test employed a secondary threshold (lower than the primary threshold used to initiate data acquisition) in order to determine whether the recorded event corresponded to direct-path propagation from source-to-sensor or was caused by multipath reflection signals. By varying the level of the secondary threshold it was possible to get either an image of the actual leak location or virtual images of the leak lying outside the AST boundary. The double-threshold approach led to accurate location estimates of 2.0-mm-diameter leaks through both the false bottom and the single bottom, as well as accurate location estimates of the leak simulator. The modified beamforming algorithm was used to develop contour maps of the signal-to-noise ratio, and these were used as the basis for determining whether a leak was present or not. The accuracy of the location estimates was within the predictions of theoretical model calculations based on the integration time and the number and location of the sensors.

4 CONCLUSIONS AND RECOMMENDATIONS

The main conclusion of the Phase III acoustic experiments is that accurate and reliable leak detection is possible; moreover, the important features of a test with high performance have been identified. It may be possible to detect leaks from holes even smaller than those used in the experiments. (It will be recalled that the three smallest holes [0.5, 1.0, and 1.5 mm in diameter] were clogged with particulates and could not be used.) The mechanism producing the impulsive leak signal (i.e., collapsing bubbles) should be independent of hole size, therefore making leaks from holes smaller than those investigated in this set of experiments detectable.

These experiments demonstrated that a detectable acoustic leak signal exists. In order to achieve reliable performance, though, significant modifications must be made to the current data collection and signal processing routines. Of the two existing types of leak signal, persistent and impulsive, only the latter can be exploited when strong multipath reflections are present in the acoustic data. These multipath signals are predictable and their presence has been verified with a simple ray-tracing model. Analysis of the experimental data shows that the multipath signals may be stronger than the direct-path signal. This finding is particularly significant because such strong multipath signals would confuse the simple threshold signal processing algorithms used for detection of the impulsive leak signal. There are a number of data collection and signal processing approaches that can be used to distinguish the direct-path from the multipath signal. One simple algorithm was developed and successfully used to detect leaks in both backfills from holes at three locations in the tank.

The success achieved with the passive-acoustic leak detection method is critically important, because until now the accepted procedure for determining whether or not an AST is leaking has been to take the tank *out of service*, drain it, and inspect the tank floor. This process is not only expensive and time-consuming but also poses environmental risks connected with the transfer and temporary storage of product. Acoustic tests have a number of important features that make them an operationally viable tool, principally in terms of minimizing interruptions to AST operations. First, the tank does not need to be taken out of service during equipment setup. Second, the test is short---it takes only a few hours to collect the data. Third, the level of product in the tank is not a factor; unlike volumetric tests, which require that the product level be lowered to within 3 to 5 ft of the bottom, no exacting level changes are needed, and a test can be conducted at the extant level. (For best performance, however, the product level should be as high as possible.)

Three general recommendations are made as part of API's Phase III effort. The first is to demonstrate that the data collection and analysis approach developed in the Phase III field tests works by using this approach to perform leak detection tests on a variety of operational ASTs whose integrity has been or will be checked by tank inspection procedures. The Phase III data are limited in that they represent only one type and size of tank, one product, and one season of the year. Although some work was done during Phase II on a 114-ft-diameter AST filled with a petroleum product, most of the acoustic experiments were conducted in the specially configured tank filled with water. Less than a month's worth of experimental data was collected, and these data are limited to ASTs in the same geographic location and under the same climatic conditions. While these experiments were carefully controlled, the data collection and analysis methods developed as part of Phase III have not yet been evaluated over a wide enough set of conditions to be definitive.

The second recommendation is to develop and validate a *standard test procedure* for evaluating the performance of acoustic leak detection methods in terms of probability of detection (P_D) and probability of false alarm (P_{FA}). The development and implementation of a standard test procedure is particularly important because it is an extremely effective means of technology transfer; it almost ensures that industry will integrate the important findings of this research into its leak detection systems, because by doing so industry can achieve the highest performance possible when evaluating these systems. Such procedures also ensure that all leak detection systems have a minimum level of performance and that the performance of one system can be compared to that of any other system. The advantages of standardized evaluation procedures, in terms of both technology transfer and performance estimation, have been successfully demonstrated and implemented as part of the underground storage tank (UST) program.

The third recommendation is to encourage the continuation of applied R & D by other organizations, especially the federal government, as a way to improve the performance of acoustic and volumetric technologies and to extend their application over a wider population of tanks. Three areas of further technology development are recommended for acoustic methods: (1) determine the presence and persistence of impulsive leak signals for a wide range of backfills and product fuels, (2) characterize the noise environment over a wider range of testing conditions, and (3) develop and evaluate more robust detection algorithms. While the goals of each of these three recommendations seem somewhat unrelated, addressing any one of them will offer significant input to the other two.

While not a specific recommendation, the importance of technology transfer cannot be overemphasized, because it must be recognized that it is expensive and time-consuming for industry to implement some of the features that have been identified as being important for achieving high performance with a passive-acoustic system. This is typically accomplished by the publication and presentation of technical results. Even more important, perhaps, is direct communication with the intended users (in this case, the commercial vendors and the owners of ASTs) for review of and comment on the test plan before each set of field tests and the test results afterward. While publication and direct interaction with the user community has been actively and vigorously pursued by API, these efforts may not be sufficient to effect the necessary changes. In our opinion, the most effective method of ensuring technology transfer involves the implementation of the second recommendation, the development of a standard test procedure.

5 IMPORTANT FEATURES OF A PASSIVE-ACOUSTIC METHOD WITH HIGH PERFORMANCE

To detect leaks in the floor of an AST, a passive-acoustic system should be designed to detect the impulsive leak signal. Off-the-shelf frequency-selective sensors that are available commercially appear to be more than adequate for this purpose.[1] For high performance, however, it is necessary to formulate data collection and signal processing algorithms that will detect this type of signal. The general features that such data collection and algorithms must possess are derived from the results of the Phase II and III field tests and analyses. The first of these features is a very high threshold; a high threshold is the best way to detect the impulsive acoustic signal produced by a leak and to minimize false alarms due to noise fluctuations. Second, digital time series of the raw acoustic wave form from each sensor must be collected and made available for analysis. Without digital data, the analysis required for robust leak detection cannot be performed. Although it would be desirable to collect continuous time histories, this would not be practical since the quantity of data collected during a normal test is prohibitively large. In effect, continuous time histories are not essential provided that each time series is sufficiently long to correctly identify the leading edge of the direct-path signal in the presence of multiple events, multipath reflections, and noise. The third important feature is an algorithm for distinguishing multipath and noise signals from direct-path signals. It is possible to devise such an algorithm because of the fact that in a high-quality threshold exceedance, the main multipath reflections relative to the direct path signal and the amplitude of the noise can be predicted. A number of approaches can be used to develop this algorithm. The fourth important feature is that the algorithm be designed in such a way that the impulsive returns from discrete bubble events are isolated and that the direct-path signals are properly time-registered. This is particularly difficult if more than one event occurs during the time it would take for an acoustic signal to propagate across the tank. The fifth feature is the spacing of sensors in such a way as to strike a balance between two opposing effects. Close spacing makes the pattern of the direct-path and multipath reflections from a single bubble event much easier to identify and thus enhances the proper identification of the direct-path signal. Unfortunately, however, as the aperture of the array decreases, so does the accuracy of the leak *location* estimates. The optimal sensor configuration (confirmed by theoretical analyses published in the literature) is thus one that addresses both issues, accurate location estimates and proper registration of impulses in the time series (Van

1 The sensors used in all field tests described here have a resonant response at approximately 30 kHz. It is likely that frequency-selective sensors that are resonant at other frequencies will also be effective, although we did not verify this. Simple laboratory tests can be used to demonstrate the response of a sensor to an impulsive signal.

Veen and Buckley, 1988). The literature indicates that an array of widely spaced sensor sets, in which each set consists of small sub-arrays of at least three closely spaced sensors, will address these issues. The sixth and final feature is that of averaging. Methods of appropriately averaging the data are needed as a way to reduce the noise and enhance the signal. In both data collection and data analysis, the approach should be to select high-quality hits and average them.

Robust leak detection requires that the time series of the raw wave form be collected digitally. The algorithms that are essential for minimizing the impact of multipath and impulsive noise require the use of such data so that the wave form before and after an impulsive event can be used in the analysis. Without digital data, none of the standard and very powerful detection methods developed for radar and sonar can be implemented. To achieve high performance, it is highly recommended that this type of data collection be implemented by industry if it is not currently being used.

There are several ways to determine whether a signal is a false alarm or a real leak signal. The first step is to simply repeat the acoustic test. This approach works well if the noise field is random and is the cause of a false alarm; if the noise is systematic or if there is some other systematic error in the method, this approach will not be particularly fruitful. The second step is to conduct another test using a completely different method, such as a volumetric test. This can be very effective because the mechanism generating the leak signal and the noise interfering with it are very different in a volumetric test than they are in an acoustic test. It is unlikely that the same false alarm mechanism will affect both methods similarly. An effective approach is to drop a hydrophone over the purported leak and listen for the strong return of the continuous signal. The presence of a signal can be determined by comparing this acoustic return to the return obtained at one or more different locations in the tank. This approach works because the strength of the signal produced by turbulent flow decays quickly as the distance from the leak increases. While this approach may be operationally inconvenient, it is a very effective way of verifying the presence or absence of a leak.

6 REPORT ORGANIZATION

The work performed as part of the Phase III program is summarized in two technical papers prepared for publication in engineering and scientific literature. The two papers appear, respectively, as Appendices A and B of this report. The paper attached as Appendix A provides a description of the signal- and ambient-noise characterization experiments and the signal-propagation simulations. The degree to which multipath propagation complicates the process of leak location is briefly discussed in this work. The paper attached as Appendix B describes the detection algorithm used to successfully locate sources of impulsive leak signals and those features of a leak detection test that are crucial to achieving high performance.

REFERENCES

Eckert, E. G. and J. W. Maresca, Jr. 1991. Detection of Leaks in the Floor of Aboveground Storage Tanks by Means of a Passive Acoustic Sensing System. *Proceedings,* 84th Annual Meeting and Exposition of the Air and Waste Management Association, Vancouver, B.C., 1991.

Eckert, E. G. and J. W. Maresca, Jr. 1992. Field Tests of Passive-Acoustic Leak Detection Systems for Aboveground Storage Tanks. *Proceedings,* 85th Annual Meeting and Exposition of the Air and Waste Management Association, Kansas City, Missouri, 1992.

Maresca, J. W., Jr., and J. W. Starr. 1990. Aboveground Tank Leak Detection Technologies. *Proceedings,* 10th Annual ILTA Operating Conference, Houston, TX, June 1990.

Van Veen, B. D. and K. M. Buckley. 1988. Beamforming: A Versatile Approach to Spatial Filtering. *IEEE ASSP Magazine.* 4:4-24.

Vista Research, Inc., 1989. *Leak Detection Technologies for Aboveground Storage Tanks When In Service.* American Petroleum Institute. Washington, D.C.

Vista Research, Inc., 1991. *An Engineering Assessment of Volumetric Methods of Leak Detection for Aboveground Storage Tanks.* API Publication No. 306. American Petroleum Institute. Washington, D.C.

Vista Research, Inc., 1992. *An Engineering Assessment of Acoustic Methods of Leak Detection in Aboveground Storage Tanks.* API Publication No. 307. American Petroleum Institute. Washington, D.C.

Vista Research, Inc., 1993. *An Engineering Evaluation of Volumetric Methods of Leak Detection for Aboveground Storage Tanks.* API Publication No. 323. American Petroleum Institute. Washington, D.C.

APPENDIX A

THE ACOUSTIC SIGNAL PRODUCED BY A LEAK IN THE FLOOR OF AN ABOVEGROUND STORAGE TANK

Eric G. Eckert and Joseph W. Maresca, Jr.

Vista Research, Inc.
Mountain View, California

THE ACOUSTIC SIGNAL PRODUCED BY A LEAK IN THE FLOOR OF AN ABOVEGROUND STORAGE TANK

by
Eric G. Eckert and Joseph W. Maresca, Jr.
Vista Research, Inc.
Mountain View, California

ABSTRACT

Acoustic leak signals produced by leaks in the floor of an aboveground storage tank (AST) were characterized as part of a field test conducted on a water-filled, 40-ft-diameter AST. In addition, the ambient noise environment encountered at the test site was characterized. The experiments were performed during May and June 1992 at a 400-tank oil refinery located in Beaumont, Texas. The impulsive component of the acoustic leak signal, caused by the interaction of air bubbles with the leak flow field, was detected in the case of both false-bottom and single-bottom backfill conditions. The leak into a well-drained, false-bottom backfill produced strong impulses with greater frequency than did a corresponding leak through a single-bottom into native-soil. Multi-path signals resulting from the reflection of impulsive leak signals within the AST interior often exceeded the direct-path impulse in amplitude. This observation was found to be consistent with the results of ray-tracing simulations applied to the AST geometry and is caused by the focusing of acoustic signals by the curved walls of the AST. An analysis of the effect of multi-path propagation on traditional acoustic leak detection systems indicates the need for careful processing of data collected through thresholding techniques. The persistent leak signal caused by turbulent flow, cavitation, and particulate collisions was found to be detectable against the background noise field at frequencies above 10 kHz. Over the range of typical sensor array dimensions this component of the leak signal did not maintain the degree of similarity that is required for accurate location of AST leaks. This lack of coherence is most likely caused by a combination of multi-path decorrelation and high ambient noise levels at frequencies below 10 kHz.

INTRODUCTION

The design of a passive-acoustic leak detection system for use on aboveground storage tanks (ASTs) must be based upon the characteristics of the leak signal and of the ambient noise against which the leak signal is measured. While laboratory simulations have addressed the nature of the leak signal and the source mechanisms that may give rise to the signal (Eckert and Maresca, 1991; Miller, 1990; Nickolaus, 1988), very little information has been published concerning the signal and noise encountered in an operational AST containing realistic leaks. Under the sponsorship of the American Petroleum Institute (API), a series of signal and noise characterization experiments were performed on a 40-ft-diameter AST located at the Mobil Oil Refinery in Beaumont, Texas, in May and June 1992.

The primary objectives of this work are to characterize the persistent and impulsive components of the acoustic leak signal observed during a one-month experimental period for leaks into two types of backfill. In addition, the characteristics of the ambient noise environment encountered under typical refinery conditions will be discussed. Finally, this work will address several aspects of signal propagation within the geometric confines of an AST that impact the manner in which leak detection systems collect and process data.

The results of the Mobil-Beaumont experiments may be summarized as follows:

- Persistent and impulsive leak signals can be detected from leaks into both false-bottom (sand) and single-bottom (native-soil) backfills.
- Ambient noise largely masks the leak signal at frequencies below ~ 10 kHz.
- Multi-path signals caused by reflections from the AST walls routinely exceeded the direct-path (leak-to-sensor) signal in amplitude. Experimental observations of multi-path signals were consistent with predictions based on a ray tracing model of acoustic propagation within the AST.
- Due to high levels of ambient noise and multi-path signal propagation, there is no statistically significant coherence between leak signals measured by spatially separated sensors.
- Detection systems based upon the persistent leak signal will not achieve adequate performance due to lack of coherence between leak signal measurements.
- Detection systems based upon the impulsive component of the leak signal must account for multi-path propagation of acoustic signals in order to achieve adequate performance.

EXPERIMENT DESIGN

The 40-ft-diameter AST used in the field tests was located at the northern edge of the Mobil-Beaumont refinery. The physical setting in which the AST was situated included many potential sources of ambient acoustic noise: roadways (one of which passed within 20 ft of the AST), leaking valves connecting steam pipes to nearby tanks, a steel recycling plant located approximately 1000 ft from the AST, and a nearby dock at which the loading or offloading of ships frequently took place. In addition to these industrial activities, natural phenomena such as wind, rain, and condensation influenced the acoustic environment in which the experiments took place.

The AST was of double-bottom construction, with a 6-in. space separating the outer bottom and the "false" or inner bottom. The space between the two bottoms was filled with sand, and the backfill beneath the outer bottom was native soil. Because the AST was being taken out of service, it could be specially configured for the experimental program. The AST had been cleaned and inspected prior to the placement of the holes in the false bottom and the installation of the hardware to control the leaks from these holes.

The water level in the tank was maintained at 25 ft throughout the experimental period. Figure 1a shows the location and diameter of 11 holes that were placed in the false bottom of the AST. Near the west edge of the tank (upper left quadrant of Figure 1a) four leaks were introduced through the use of carburetor jets tapped into the false bottom. These four leaks

(a)

HOLE	D (mm)	BACKFILL
3.0-S	3.0	Sand
2.0-S	2.0	Sand
1.5-S	1.5	Sand
1.0-S	1.0	Sand
0.5-S	0.5	Sand
3.0-C	3.0	Native Soil
2.0-C	2.0	Native Soil
1.5-C	1.5	Native Soil
1.0-C	1.0	Native Soil
0.5-C	0.5	Native Soil
SIM	3.0	Native Soil

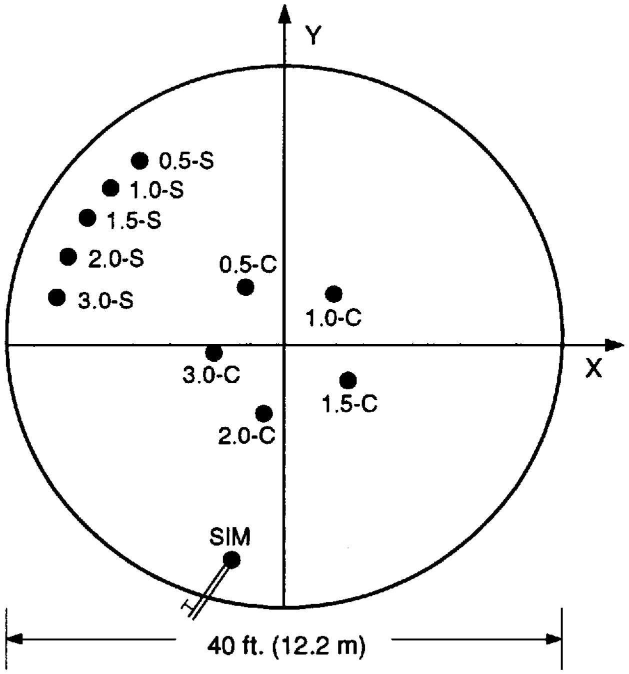

(b)

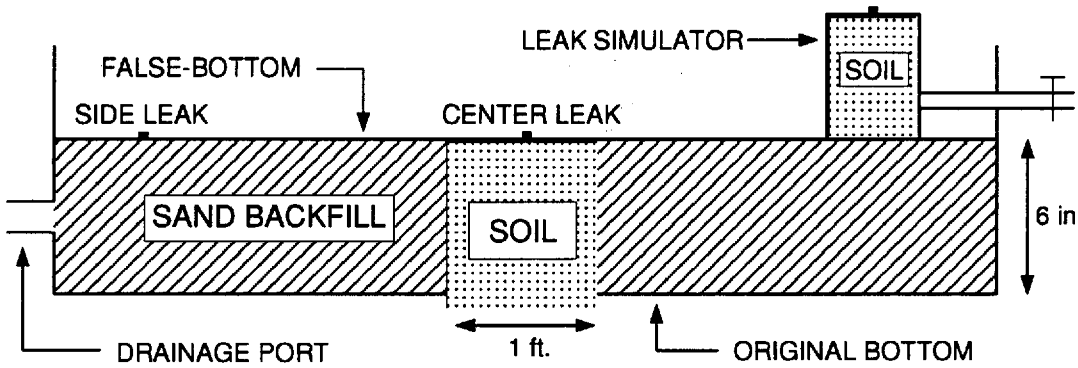

Figure 1. (a) Location and diameter of holes installed in 40-ft-diameter AST. Side holes (S) leak through false-bottom (sand backfill); center holes (C) leak through single bottom (native-soil backfill). Simulator (SIM) flow rate controlled by valve external to AST. (b) Backfill conditions for the side and center leaks and the leak simulator (not to scale).

were equivalent to leaks from holes with diameters of 0.5, 1.0, 1.5 and 2.0 mm, respectively. A fifth hole 3 mm in diameter was drilled directly into the steel of the false bottom. Leaks from all five holes were allowed to drain into the 6-in.-thick sand backfill located in the space between the false and outer bottoms. A similar set of five holes was placed near the center of the tank. While the holes were the same size as those along the west edge of the tank, the backfill into which the center leaks drained was quite different. Beneath each of the center holes, a 1-ft-diameter, 6-in.-deep section of the sand backfill had been removed and replaced with the native soil found at the refinery. Finally, near the south edge of the AST (the lower left quadrant of Figure 1a), a leak simulator was welded onto the false bottom. The simulator consisted of a 1-ft-diameter steel cylinder capped at both ends and fitted with a 3-mm-diameter

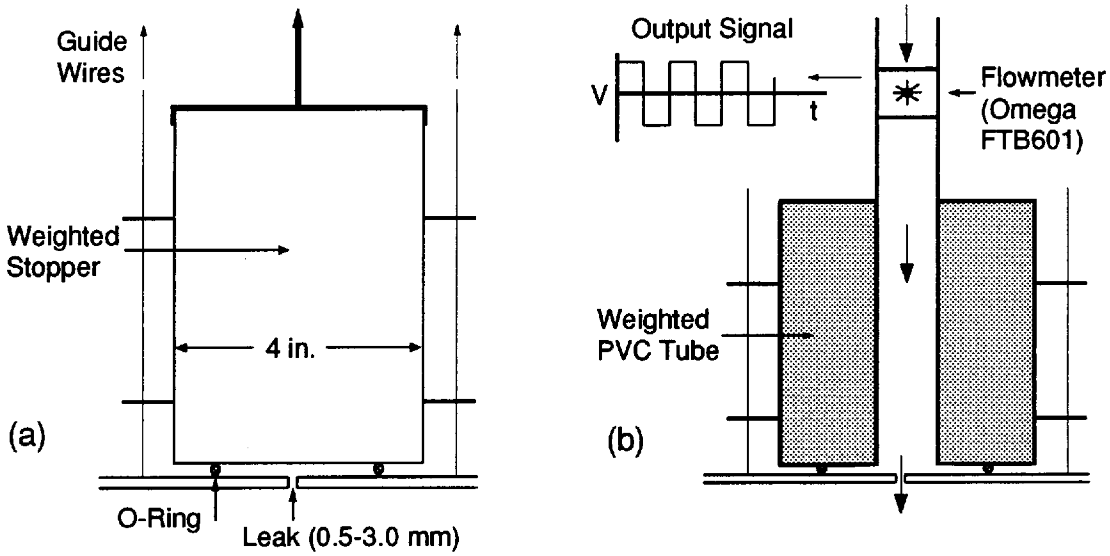

Figure 2. (a) Stopper designed to control leaks. Leak status was monitored by a hydrophone placed near the hole. (b) Flow meter capable of measurements from 1 to 30 gal/h.

hole. Native soil was used as the backfill within the simulator. The output of the simulator drained out via a pipe through the wall of the AST. The flow rate for leaks induced with the simulator was controlled by means of a valve external to the AST. The backfill conditions beneath the center and side leaks and within the leak simulator are shown in Figure 1b.

Figure 2a shows the device used to turn leaks on and off. These leak stoppers were constructed of PVC tubing closed off at both ends and weighted with a mixture of cement and lead shot. O-rings were used to provide a water-tight seal between the stopper and the tank floor. Verification that a leak was off was provided by a hydrophone placed approximately 4 in. from the hole. Figure 2b shows an Omega-FTB601 flow meter, the instrument used to measure the flow rate associated with the leak from each hole. The flow meter was powered by a 12-volt power supply located on the AST roof. The square wave output of the flow meter was monitored with an oscilloscope. Calibration tests with the leak simulator showed that the flow meter produced accurate measurements of flow rates between 1 and 30 gal/h with a precision of ± 1 gal/h.

The locations of the internal and external acoustic sensors are shown in Figure 3. The sensors chosen for the experiment were CTI-30, 30-kHz resonant piezoelectric transducers. While the CTI-30 is primarily designed for acoustic emissions applications (due to the resonant response near 30 kHz), the transducer is also quite sensitive at audio frequencies (DC-20 kHz). The external sensor array consisted of 12-elements, and was arranged in three sub-arrays of 4 elements each. The sub-arrays were located at 0°, 60°, and 120° degree angular positions on the AST circumference. The element spacing within each sub-array was 1.5 ft. The 7-element internal sensor array was deployed down a 3-ft-diameter manway located near the northeast edge of the AST. The spacing for elements of the internal array was approximately 1.5 ft.

A diagram of the data acquisition system used in the collection of experimental data is shown

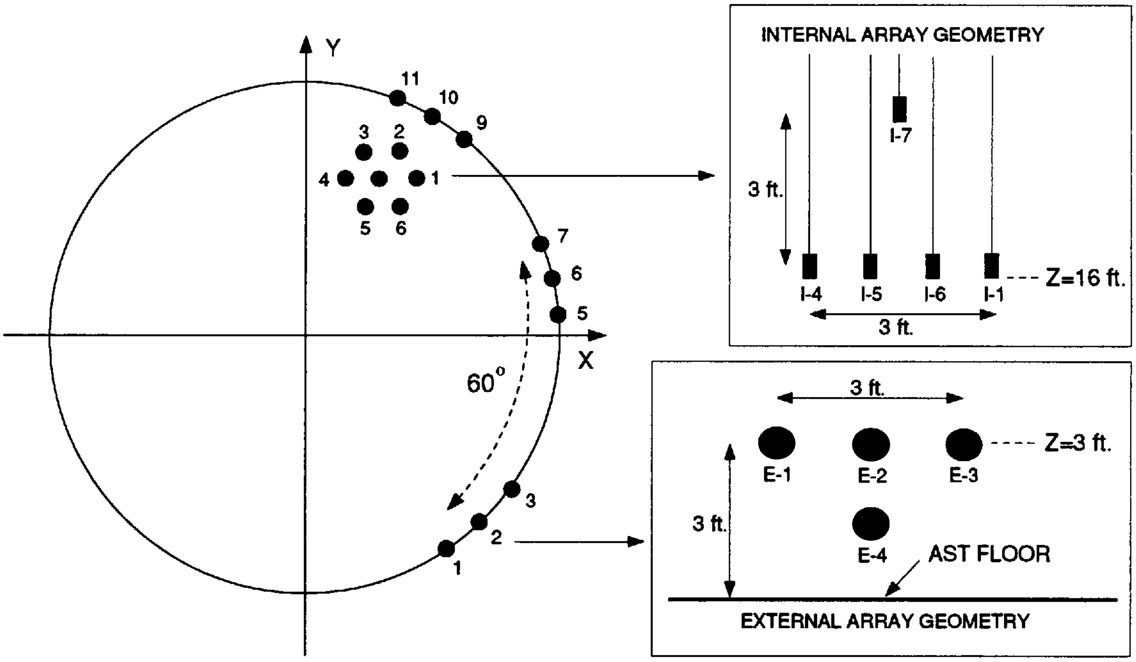

Figure 3. Geometry of 7-element internal and 12-element external sensor arrays (not to scale).

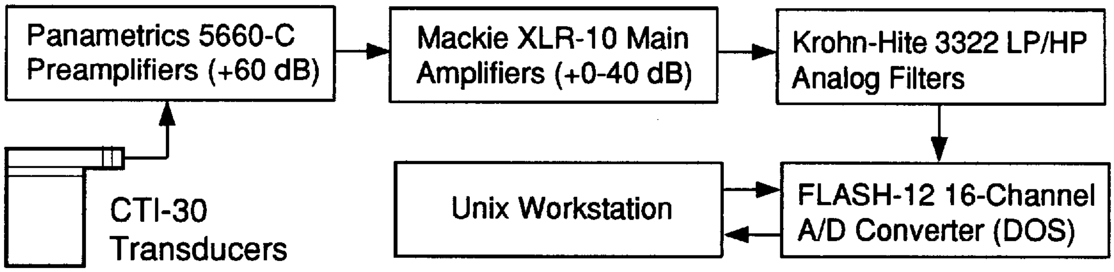

Figure 4. Diagram of the data acquisition system used in the experiments. The digitization card is capable of simultaneously sampling 16 channels at 62.5 kHz. System noise level is extremely low.

in Figure 4. The output of each CTI-30 transducer was amplified by approximately +100 dB in two stages by Panametrics 5660-C preamplifiers and Mackie XLR-10 main amplifiers. The amplified signals were filtered using Krohn-Hite 3322 analog filters. Filtering was either low-pass (DC $\leq f \leq 31$ kHz) for acquisition of low-frequency signals, or high-pass ($f \geq 15$ kHz) for acquisition of high-frequency, impulsive signals. The analog signals were digitized by an STI Flash-12 data acquisition board housed in a DOS micro-computer. Data analysis and the initiation of data collection were controlled by a Unix workstation that was linked to the DOS computer through a local network. The combination of sensors and amplifiers chosen for the experiment resulted in a very low level of system noise. Acquisition of 16-channel data at sampling frequencies up to 62.5 kHz was possible.

THE AMBIENT NOISE ENVIRONMENT

Measurements of AST acoustic leak signals are generally made against an ambient noise field that is highly variable both in strength and frequency distribution. The complex variety of noise sources encountered at a refinery ensures that acoustic data recorded within any frequency band and over any time scale will be subject to some form of contamination by ambient noise. Sources of persistent acoustic noise (i.e., noise that is typically present during all measurement periods) include industrial activities associated with the refinery and nearby factories, traffic, and leaking valves in aboveground steam-distribution pipelines. While these sources produce consistently high levels of ambient noise, the frequency content of persistent noise is largely confined below ~ 10 kHz.

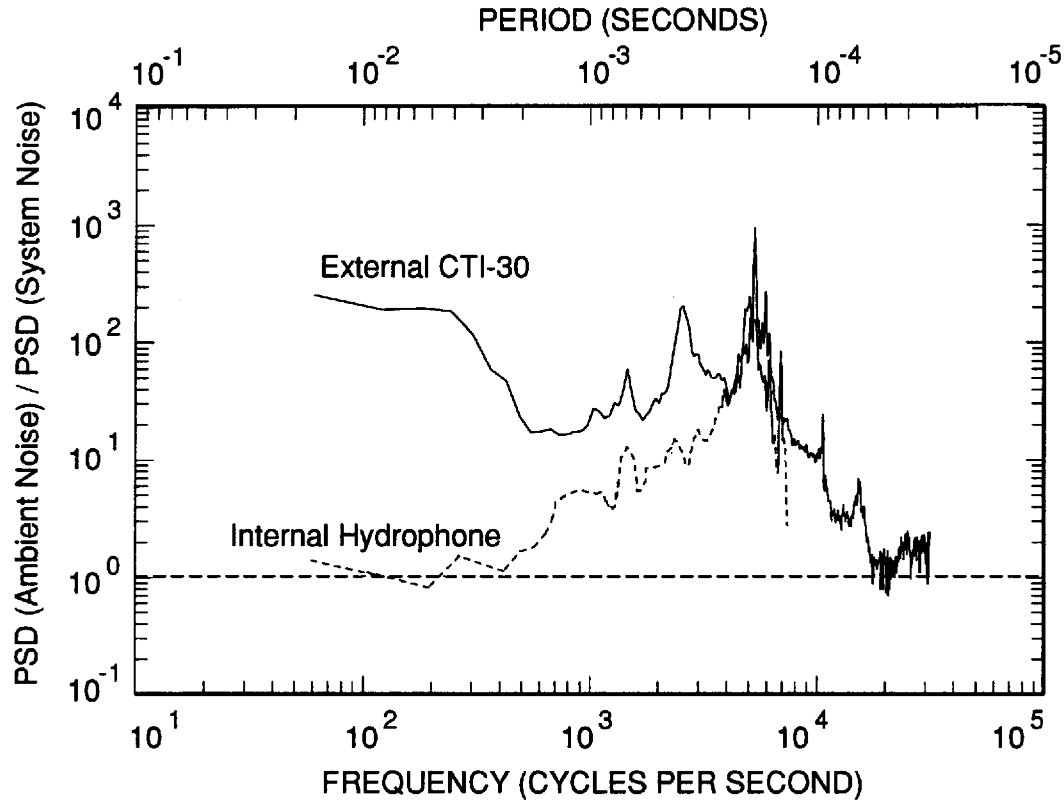

Figure 5. Power spectral density of ambient noise normalized against the system noise. The solid line shows PSD measured by the 12-element array of external sensors; the dashed line shows PSD measured by an internal hydrophone. The hydrophone was located 3 ft above leak 3.0-C.

Figure 5 shows the power spectral density (PSD) of ambient acoustic noise measured by external sensors and an internal hydrophone during a 10-min period judged to be relatively quiet. The hydrophone PSD bandwidth reflects the limited (10-6000-Hz) frequency response of the transducer. The spectral plots are normalized against the system noise level and are based upon 50 time series of 100-ms duration each. On average, ambient noise is most severe at frequencies below 10 kHz and drops off sharply at frequencies above 10 kHz.

Sources of distinctive, impulsive noise (i.e., noise that occurs infrequently and is localized in

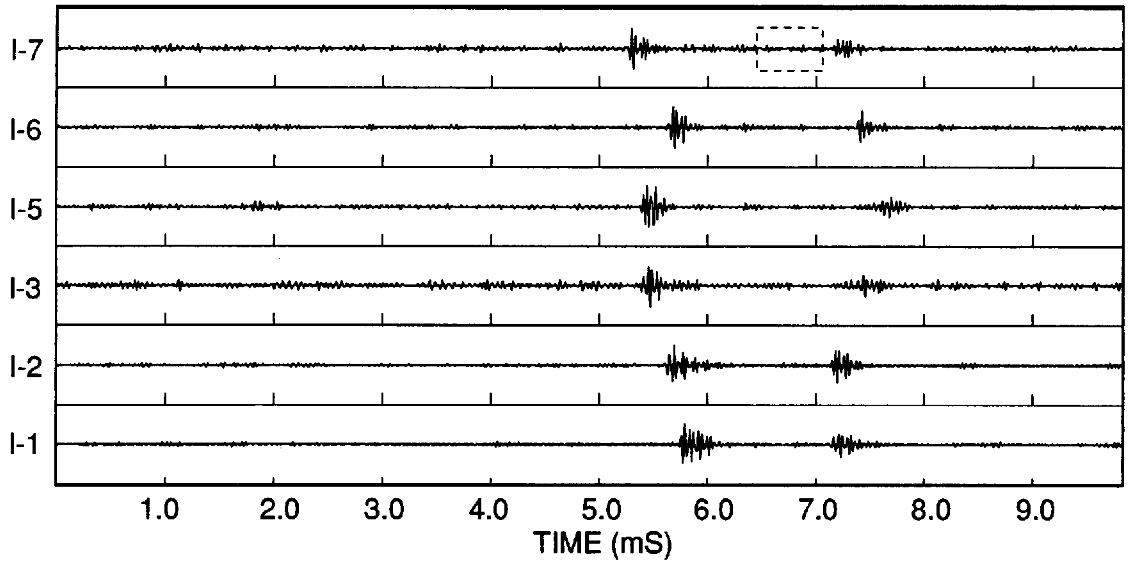

Figure 6. Condensation impulse recorded by a 6-element, narrow-aperture internal array. A secondary impulse resulting from reflections within the AST interior is also detected.

time) are also observed as part of the AST ambient noise environment. Mechanisms observed to cause impulsive noise included rain, condensation, and mechanical stresses imparted to the AST through connecting pipelines during product transfers. Resonant sensors, such as the CTI-30, respond to broadband, impulsive signals by briefly ringing at the sensor's resonant frequency. Figure 6 shows time series of a condensation drip measured by a 6-element, narrow-aperture internal array. Element I-7 of the internal array lies 3 ft above the horizontal plane containing the remaining elements. Based on the array geometry, tank diameter, product height, and sound speed, the dashed box shown in Figure 6 indicates the arrival-time window within which the I-7 impulse would have appeared had it originated from any point on the AST floor. While impulsive noise sources can often be avoided through careful choice of measurement period and sensor location, the magnitude of impulsive noise is generally large in comparison to that of persistent noise sources.

THE ACOUSTIC LEAK SIGNAL IN AN AST

Through the use of laboratory simulations, four source mechanisms have been identified that give rise to the acoustic leak signal (Eckert and Maresca, 1991). Turbulent flow and cavitation produce a continuous, low-frequency ($\leq$ 10 kHz) signal that is believed to persist for a large class of AST leaks. Leaks into backfill materials that contain small-diameter particulates, such as sand, produce a continuous, broadband component of the leak signal. Finally, if the backfill material contains entrapped air bubbles, these bubbles may interact with the leak flow field to produce a large amplitude, impulsive leak signal. The rate at which impulses are emitted via the entrainment of air into the leak flow field depends on the amount of air in the vicinity of the leak.

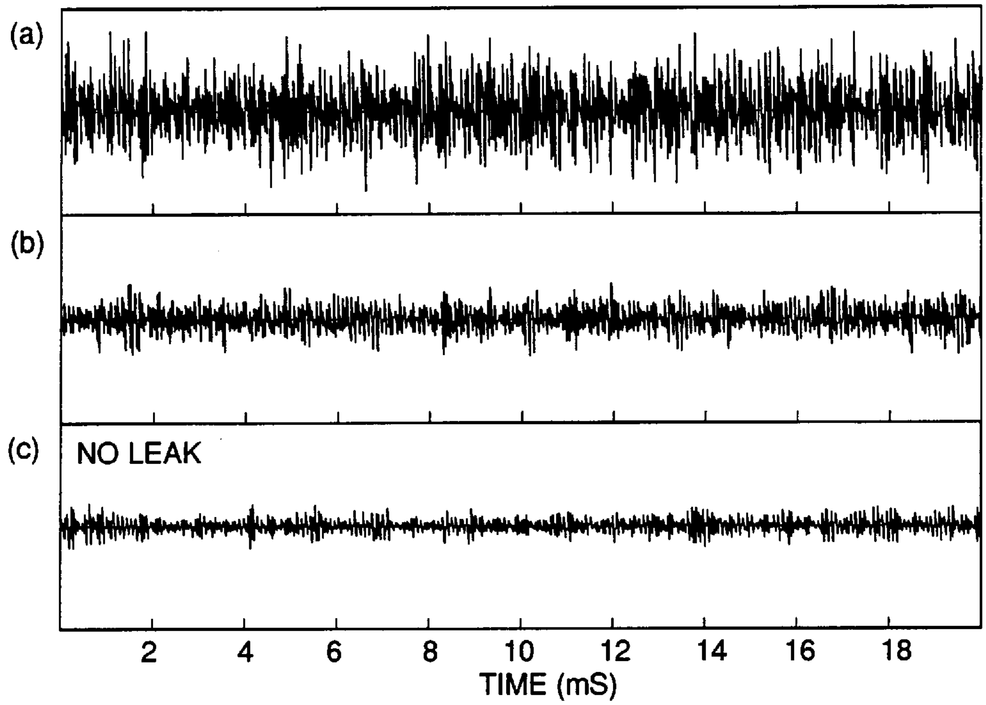

Figure 7. Time series of the persistent leak signal produced by leaks into (a) false-bottom (sand backfill), and (b) single-bottom (native-soil backfill). Time series (c) was recorded under no-leak conditions. Sensors are externally mounted; leak-sensor separations are 30 ft (a) and 25 ft (b).

The characteristics of the leak signal produced by a 2.0-mm-diameter hole were investigated by means of a variety of internal and external sensor configurations. The smaller holes installed as part of this experiment (0.5, 1.0, and 1.5 mm in diameter) produced no measurable flow and were presumed to be clogged with debris. The lack of flow through the holes was verified with the flow meter and the hydrophone. Figure 7 shows time series of acoustic leak signals recorded by external sensors in the presence of leaks into the false bottom (sand backfill) and through the single bottom (native soil backfill). The hole diameter was 2.0 mm in both cases and the distance between the leak and the sensor was 30 ft in the case of the false bottom and 25 ft in the case of the single bottom. A reference time series recorded prior to the initiation of the leaks is also shown. The measured flow rate for both leaks was between 15 and 20 gal/h. Thirty data sets of 60-ms duration each were recorded at a sample frequency of 62.5 kHz over a period of approximately 10 minutes. Data shown in Figure 7 have been high-pass filtered to eliminate ambient noise at frequencies below 5 kHz.

Several important observations can be made regarding the time series in Figure 7: (1) the leak into the false-bottom containing well-drained sand emits a much larger signal than a corresponding leak through a single-bottom into native soil, (2) the false bottom leak is clearly detectable against the ambient noise level, and (3) during this particular 60-ms collection interval, no large-amplitude, impulsive events were measured. For comparison, Figure 8 shows the single realization of the 30-data-set ensemble in which an impulsive event was emitted by the false-bottom leak. The magnitude of the impulsive signal is large in comparison to both the

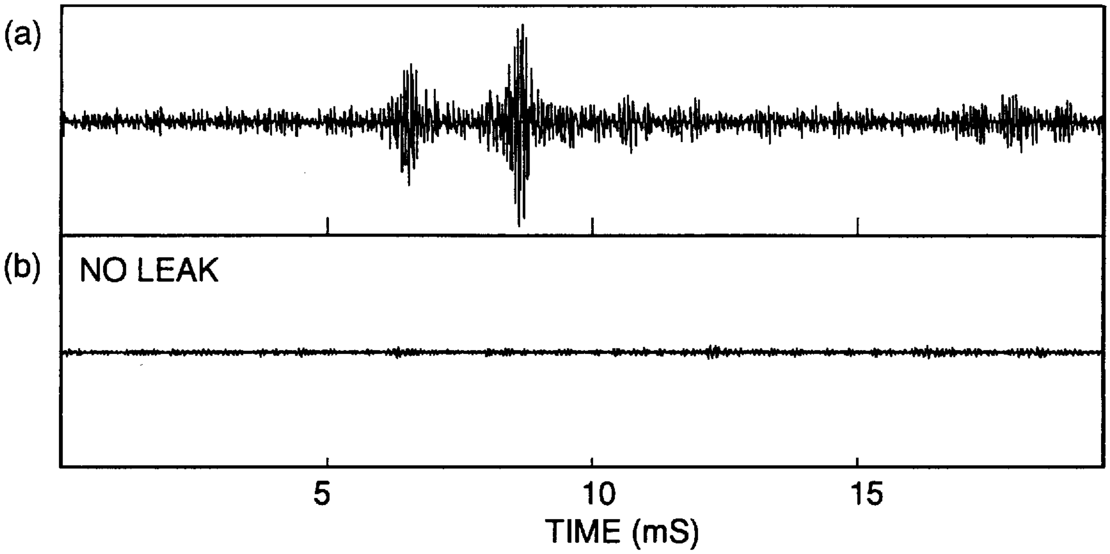

Figure 8. Time series of impulsive leak signal emitted by 2.0-mm-diameter leak into sand backfill. Within the entire two-second record, a single impulsive event was observed. A no-leak time series is shown for reference.

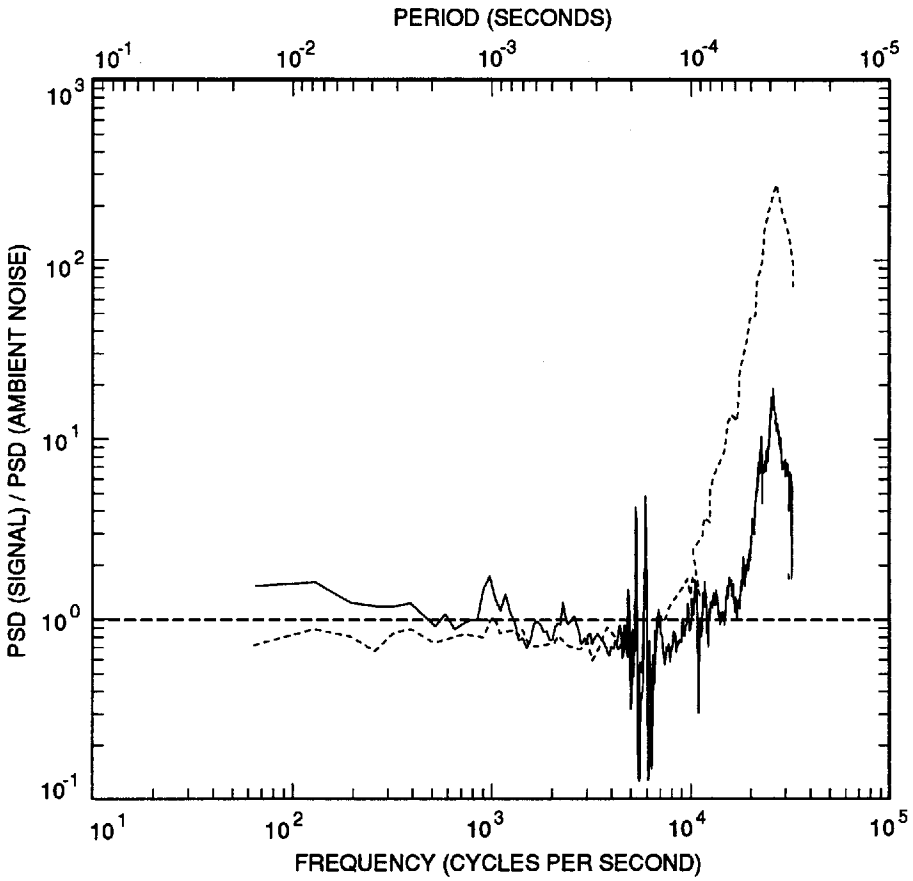

Figure 9. PSD of persistent leak signal normalized against PSD of ambient noise for a 2.0-mm-diameter leak into native-soil backfill (solid line) and sand backfill (dashed line). Sensors are externally mounted; distances between the leak and the sensor are 30 ft (sand backfill) and 25 ft (native-soil backfill).

ambient noise level and the persistent component of the acoustic leak signal.

Three differences exist between the two backfills that may account for the observed dissimilarities in the strength of the persistent leak signal. The sand backfill installed between the two tank bottoms was very well drained; several drainage ports surrounding the AST remained open throughout the experiment. A well-drained backfill contains much more air than a saturated backfill, and so the signal enhancement could be due to the continuous entrainment of air by the false bottom leak flow field. Also, the sand beneath the false bottom leak may be more easily entrained into the turbulent leak flow field than is the case for the native-soil backfill. Thus, particulate collisions could play an important role in generating the false bottom acoustic leak signal. Finally, the close proximity of the false bottom leak to the tank wall, combined with the use of an externally mounted sensor, allows a substantial portion of the leak signal to reflect off of the AST wall and into the receiving sensor. This multi-path effect will be explored in greater detail in the next section.

Figure 9 shows a plot of the power spectral density of the 2.0-mm-diameter persistent leak signal normalized against the ambient noise PSD. Each PSD represents an average of 210 1024-point FFTs individually detrended and weighted with a cosine bell. A signal-to-noise ratio (SNR) of 1 is indicated by the dashed line. Due to the high level of ambient noise, the signal-to-noise ratio is approximately unity up to a frequency of 5 to 10 kHz. The large fluctuations in the measured SNR between 4 and 7 kHz are caused by variations in the ambient noise field associated with a nearby factory. The strong peak in both spectra occurring near 25 kHz reflects the resonant response of the CTI-30 transducer. At frequencies above 10 kHz, the false-bottom, sand-backfill SNR exceeds the SNR of the single-bottom leak by a factor of 10. However, viewed in the frequency domain, the persistent leak signal into native soil is still clearly detectable, even against a relatively strong ambient noise field.

Use of the persistent component of the acoustic leak signal to detect AST leaks requires that a high degree of similarity be maintained between signals received at spatially separated sensor locations. The complex coherence function, which is a measure of signal similarity as a function of frequency (Carter, 1987), was computed for pairs of time series measured by internal and external sensors at a variety of sensor separations. No statistically significant coherence was observed for any sensor pair, even at separations of only 6 in. This result implies that the differential arrival time of the persistent leak signal at spatially separated elements of a sensor array cannot be reliably measured. The lack of coherence is caused by: (1) high levels of ambient noise at frequencies below 10 kHz, (2) variations in individual sensor output with respect to similar input at frequencies near the transducer resonance, and (3) the reception of multi-path signals along with the direct, leak-to-sensor signals. The observed lack of signal similarity, even for the relatively strong leak signals produced by the false bottom leak, imply that the persistent leak signal is not a viable candidate for the detection of AST leaks, and must instead be viewed as a source of noise. While an array of sensors positioned far from the leak source is incapable of detecting the persistent leak signal, a sensor in close proximity to the leak will record a measurable difference in signal strength in

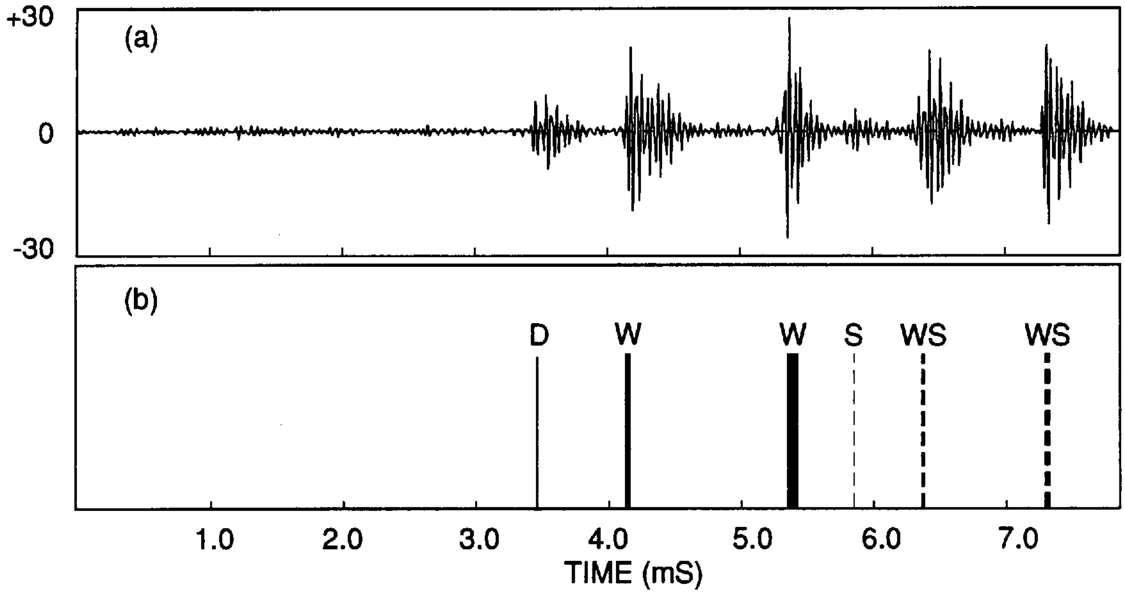

Figure 10. (a) Time series of impulsive acoustic leak signal produced leak into false-bottom (sand) backfill. Sensor is an internal CTI-30; amplitude scale is in multiples of rms noise level. (b) Simulated arrival times of reflection signals relative to direct-path signal (D). Dashed line indicates reflection from air/water interface.

comparison to the ambient level. Thus, an acoustic sensor moved to a specific location on the AST floor can use the persistent leak signal (flow noise) to verify a suspected leak.

IMPULSIVE ACOUSTIC LEAK SIGNALS IN AN AST

The large-amplitude, impulsive component of the acoustic leak signal was observed in the presence of false bottom, single bottom, and simulated leaks. Based upon the collection of impulsive events using a trigger threshold of $\sim$ 20 to 50 times the root-mean-square (rms) noise level, leaks into the false bottom of the AST were observed to produce the greatest frequency of impulsive events (typically 1 to 20 per minute), while leaks through the single bottom into the native soil backfill emitted impulses at a greatly reduced frequency (typically 1 every 5 minutes). The production of impulses by the leak simulator was controlled by the amount of air injected into the backfill cavity prior to the initiation of flow. The leak flow rate through the simulator, which was between 2 and 20 gal/h, was observed to have no effect on the rate of impulse emission. The impulsive leak signal appears to be detectable for realistic AST leaks, it is much larger in amplitude than the persistent leak signal, and it is less subject to contamination by persistent noise sources typically encountered at a refinery. These three facts point toward the impulsive leak signal as the most likely candidate for the successful detection of AST leaks.

Figure 10a shows a time series recorded by one member (I-5) of the 7-element internal array during an experiment in which the 2.0-mm-diameter leak into the false-bottom backfill was active. Prior to digitization, the analog signal was high-pass filtered with a cutoff frequency of

15 kHz; the digitization frequency was 62.5 kHz. The predicted times at which multi-path impulses are received by the transducer relative to the direct-path impulse (i.e., the signal that propagates along a direct path from leak to sensor) are indicated in Figure 10b. The arrival times for multi-path signals were computed using a ray-tracing program that accounted for single and double reflections of emitted impulses off the AST's side walls or from the air/water interface. Line thicknesses for the multi-path signals of Figure 10b are drawn in proportion to the number of simulated rays intersecting the sensor volume. The four propagation paths shown are source-sensor (D), source-wall-sensor (W), source-surface-sensor (S), and source-wall-surface-sensor (WS). The data for the time series of Figure 10a were collected with a trigger threshold set at approximately 20 times the rms noise level; the amplitude has been scaled such that the rms noise level is equal to 1. Several important observations can be made regarding signal propagation in ASTs based upon the data of Figure 10: (1) all of the impulsive signals present in the time series are caused by the emission of a single impulse at the leak location, (2) arrival times for multi-path signals are consistent with a simple ray-tracing model that assumes the AST to be a perfectly reflective cylinder, and (3) because of focusing by the curved AST walls, the amplitude of multi-path signals can be larger than that of the direct-path signal. The relatively small amplitude associated with the source-surface-sensor (S) propagation path is due to the fact that no focusing occurs at the air/water interface. Given that multi-path signals are strong and numerous, an understanding of the propagation of impulsive signals within the geometry of an AST is important with regard to the design of acoustic leak detection systems.

ARRAY MEASUREMENTS OF THE IMPULSIVE LEAK SIGNAL

Time series of an impulsive event recorded by a 6-element array of closely spaced internal sensors and a 6-element array of widely spaced external sensors are shown in Figure 11. The source of the impulse was the leak simulator in which a 2-gal/h flow into a partially saturated backfill was established. The trigger threshold set to initiate data acquisition was approximately 25 times the rms noise level. A ray-tracing simulation based upon the known source and sensor locations again shows that the impulses present in Figure 11 are consistent with reflections of a single impulse off the AST's side walls. The presence of multi-path signals and the amplitude of these signals relative to the primary signal is a function of both source and sensor location. Sensors E-1 and E-3 of Figure 11 receive relatively little multi-path signal in comparison to the other array elements. If the sensor array of an acoustic leak detection system is spread over a wide aperture, it is likely that the degree of multi-path contamination will vary substantially among the individual array elements. Even if the elements of an acoustic array are closely spaced (e.g., the internal array elements of Figure 11, which are spaced between 1.5 and 3.0 ft from one another), temporal and amplitude variations in multi-path signal produce time series that, after the primary impulse is received, are surprisingly dissimilar.

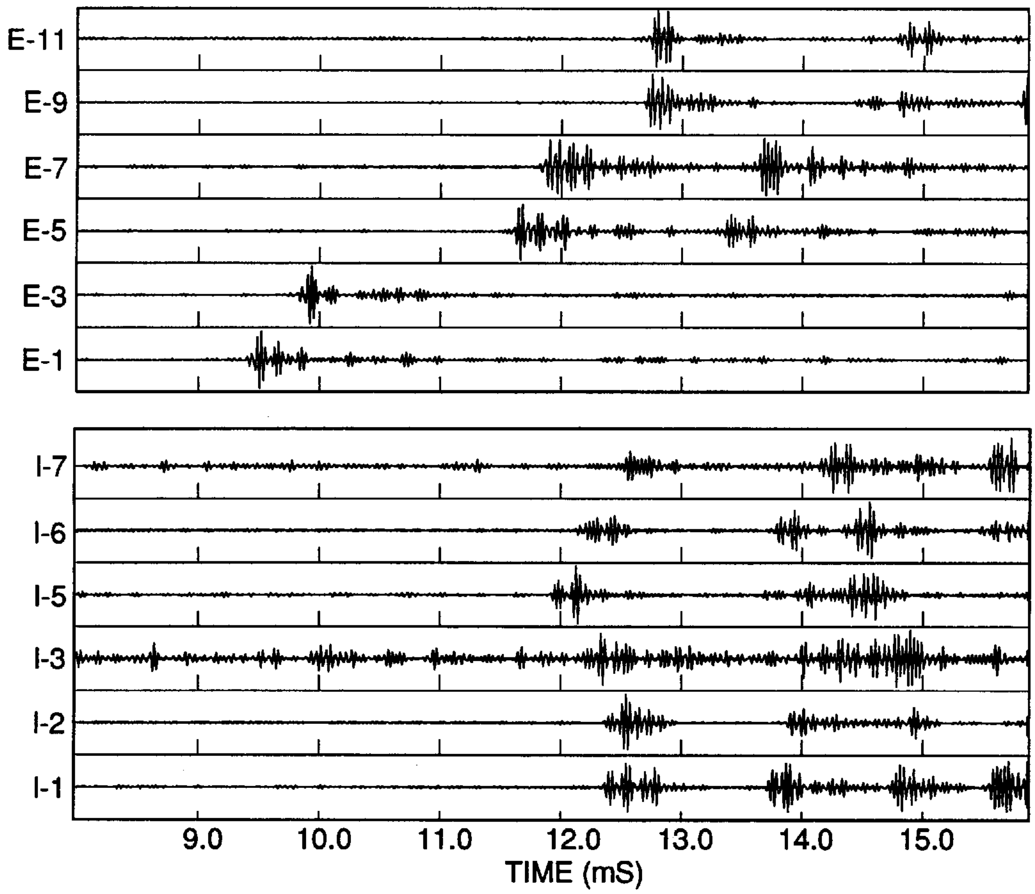

Figure 11. Time series of impulsive leak signal measured by 6-element internal and 6-element external arrays. The leak signal was emitted by the leak simulator under 2 gal/h flow. Trigger channel is I-1; sampling frequency is 62.5 kHz.

The ray-tracing simulation can be used to identify regions of the AST floor that will subject a sensor at a specified location to severe multi-path contamination. Simulation of the impulse-response of the AST proceeds as follows: (1) the sensor location is specified, (2) an (x,y) grid of source locations (typically 5000 points) is established on the AST floor, (3) a large number of rays (typically 10^5) are propagated from each source location into the half-space above the AST floor, and (4) the arrival times of rays that intersect the sensor volume after zero (direct-path) or one (multi-path) reflections from the AST walls or air/water interface are computed. One measure of the strength of multi-path signals compared to that of direct-path signals is to form a ratio between the number of multi-path rays received by the sensor within a narrow window ($\sim$ 0.5 ms in width) and the number of rays received via the direct path. A ratio of unity indicates that at some time after the direct signal is received, it is expected that a multi-path signal of approximately equal amplitude will arrive. Figure 12 shows a contour plot of the multi-path impulse response of an external sensor whose distance above the tank floor is 5% of the tank diameter. The contour labels indicate the value of the multi-path/direct-path ratio as a function of source position. If an impulsive source is located

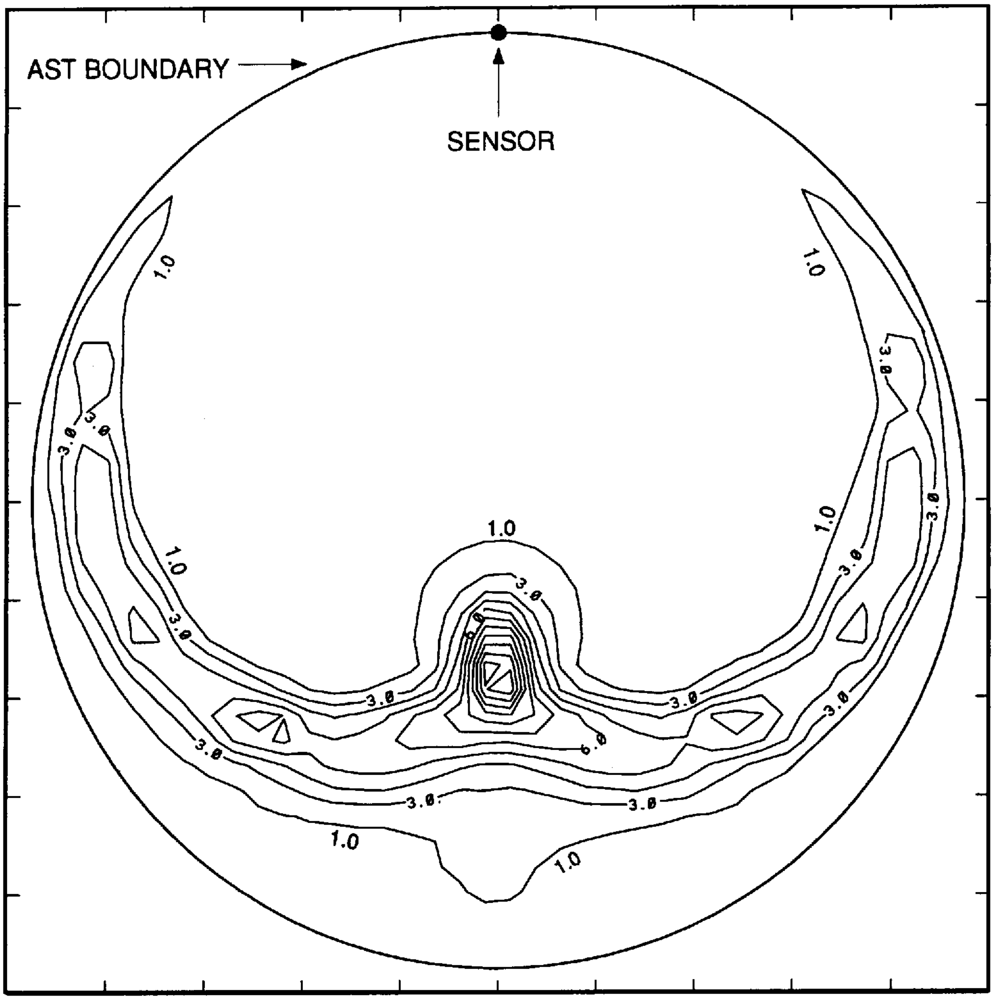

Figure 12. Impulse-response of an external transducer as a function of source location on AST floor. Contour intervals represent ratio of number of multi-path impulses received to number of direct-path impulses received within a 0.5-ms window. Contour labeled 1.0 bounds the source-location region for which strong multi-path signals are expected.

anywhere within the contour labeled 1.0, it is expected that the strongest received signal will result from multi-path reflections rather than direct leak-to-sensor propagation. While the region of severe multi-path contamination for a *single*, external sensor represents a relatively small fraction of the AST floor area, the multi-path problem must be considered in the context of an array of sensors. In order to spatially locate the source of a signal, it is desirable to have many sensor elements spread over a wide aperture (i.e., over a significant fraction of the AST's circumference). If the array contains a reasonable number of elements (e.g., 8) and covers an aperture suitable for accurate location (e.g., 120°), Figure 12 suggests that some elements of the array will be subject to severe multi-path contamination for any source location.

SOURCE LOCATION AND MULTI-PATH PROPAGATION

The strong multi-path signals associated with the AST geometry complicate the design of a robust leak detection system based upon the impulsive leak signal. Because the impulsive leak signal appears infrequently and must be sampled at a high frequency (in order to avoid persistent ambient noise), information is provided to the detection system only when a preset threshold signal level is exceeded at one or more sensor locations. Whether this information consists of time series of sufficient length to contain the impulse of interest, or merely the arrival time of the impulse at each array element, the quality of a given measurement is strongly dependent upon the ability of the system to (a) process only information that originates from a single event (i.e., the emission of a single impulse), and (b) discriminate between information propagated along direct paths from source to sensor and multi-path propagation. The manner in which a leak detection system may achieve these data quality objectives is discussed in greater detail in Appendix B. In order to illustrate the need for further refinement of the data collection and processing used by AST acoustic leak detection systems, the time series pictured in Figure 13 will be analyzed in the context of source location.

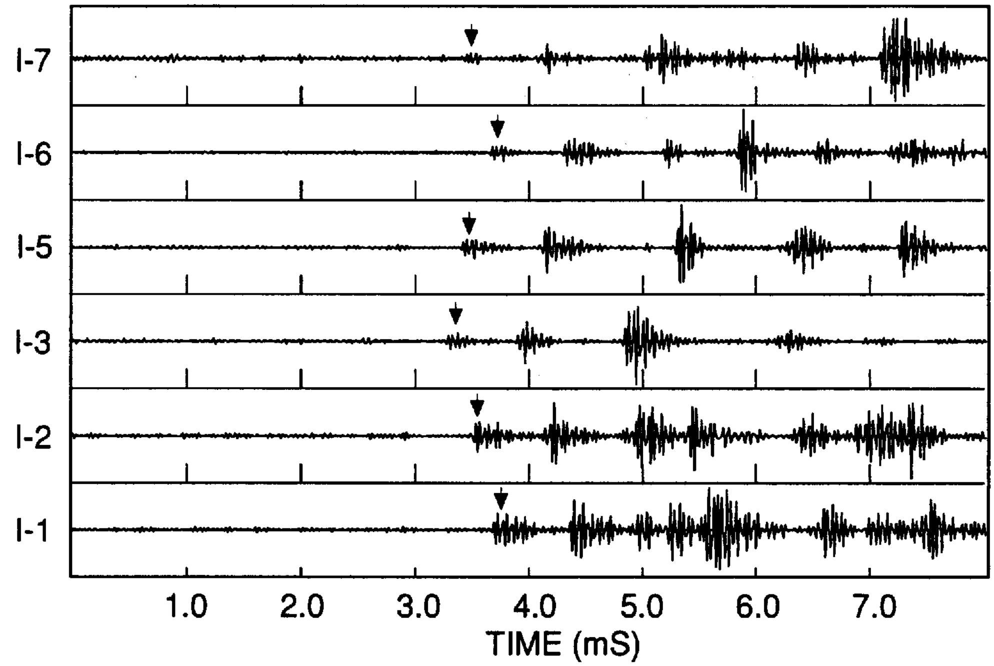

Figure 13. Time series of an impulsive leak signal measured by a 6-element, narrow-aperture internal array. Source is leak 2.0-S (false bottom leak); arrows indicate arrival of direct-path impulse. Vertical position of all array elements was the same (z=16 ft) for this measurement.

Figure 13 shows time series of an impulsive event emitted by the 2.0-S leak into the false bottom of the AST. The threshold signal level used to collect the time series was approximately 20 times the rms noise level. The measured arrival times of the direct-path impulse (indicated by arrows in the figure) are consistent with the known location of the leak. The relative position of the leak and the 6-element, narrow-aperture array are such that the multi-path signals are generally much stronger than the direct-path signal. If the detection system is designed to measure the time at which a preset threshold is exceeded at each array element, the time series of Figure 13 can be used to estimate the range of threshold settings such that the measured arrival times correspond to the reception of the direct-path signal. A simple calculation shows that in order to accurately locate the source of this *particular* event, the threshold signal level must be set within the range $3 \leq V_T/V_n \leq 8$, where V_T is the threshold level and V_n is the rms noise level computed from data preceding the direct-path impulse. The lower bound on the threshold range is determined by the maximum observed noise fluctuation; the upper bound is determined by the largest threshold that will allow for the collection of direct-path arrival times by all of the elements of the sensor array. If the threshold is set between $8 \leq V_T/V_n \leq 35$, the set of impulse arrival times collected will be contaminated by multi-path signals. Threshold settings above 35 V_n result in no data collection.

The use of a threshold exceedance to initiate data collection is demanded by the nature of the impulsive leak signal. This calculation suggests that data acquired in such a manner will frequently supply information to the detection algorithm that is contaminated by multi-path signals. In order to correctly interpret data collected at any threshold setting, the detection algorithm must recognize multi-path signals as an important component of the acoustic leak signal.

CONCLUSIONS

Acoustic leak signal and ambient noise characterization experiments performed as part of a field test on a 40-ft-diameter AST produced several important results. Impulsive and persistent components of the leak signal were found to be detectable in the case of leaks from 2.0-mm-diameter holes through the false bottom (sand backfill) and single bottom (native-soil backfill) of the AST. The persistent ambient noise encountered at the Beaumont Refinery was greater in magnitude than the persistent leak signal at frequencies less than $\sim$ 10 kHz. At frequencies greater than 10 kHz, leaks into both backfill materials produced signals that were detectable over the AST dimensions. The coherence between persistent leak signals recorded by closely spaced acoustic sensors was observed to be below the level of statistical significance required in order to accurately measure the differential arrival time of the signal. It was concluded that the lack of coherence was caused by high levels of ambient noise and the propagation of multi-path signals within the reflective interior of the AST. The inability to measure the relative arrival time of leak signals at spatially separated sensors implies that the persistent leak signal is not a viable candidate for the detection of AST leaks, and must instead be viewed as a source of persistent noise.

Impulsive leak signals caused by the interaction of air bubbles with the turbulent leak flow field were observed for leaks into both backfill materials and through a leak simulator. The frequency of large-amplitude impulse emission was found to be much greater for the false-bottom leak (~ 1 to 20 per minute) than for a leak through the single-bottom into native soil (~ 1 per 5 minutes). A ray-tracing simulation designed to predict the arrival time of multi-path signals caused by reflections was used in the analysis of measured impulsive leak signals. General agreement was observed between predicted and measured values of the multi-path impulse arrival time and amplitude relative to the direct-path signal. The nature of the multi-path signal produced by an impulsive leak signal was found to be strongly dependent upon the source and sensor locations. Simulation of the impulse response of an external sensor to a collection of sources distributed over the entire tank floor showed that wide-aperture external sensor arrays will be subjected to some degree of multi-path contamination regardless of the leak's location.

A brief discussion of the effect of multi-path propagation on the leak location procedure showed that the manner in which data are collected (threshold exceedance) cannot avoid the contamination of data sets by multi-path signals. That this method of data collection is required, due to the infrequent occurrence of leak impulses, points out the need for careful processing of the leak signal by the leak location algorithm.

RECOMMENDATIONS

The complete characterization of the acoustic signal produced by leaks in the floor of an AST requires that three additional experiments be performed. While the experiment described in this work was conducted over a one-month period, there is still some question as to whether the impulsive leak signal diminishes with time, and whether this signal is produced under a wide variety of backfill conditions. Also, the relationship between the impulsive leak signal and the leak flow rate should be quantified. A relatively simple experiment that addresses each of these concerns could be performed on a small-diameter test tank.

Multi-path signals comparable in amplitude to the direct-path signal, and the problems that such signals may present to a leak location algorithm, have been described in the context of measurements conducted on a small (40-ft-diameter) AST. The degree to which multi-path signals are present in large-diameter tanks should be investigated. This experiment does not necessarily require that real leaks be induced in large tanks, but could instead be accomplished by placing a broadband acoustic transmitter within the AST.

The acoustic leak signal must eventually be characterized for the variety of products typically stored in ASTs. The relationship between leak signal and product type can be investigated either through the use of a laboratory leak simulator, or by installing leak simulators such as that used in this work into operational ASTs.

ACKNOWLEDGEMENTS

The authors wish to gratefully acknowledge the cooperation of Mobil Oil Company, and in particular John Collins of the Beaumont Refinery, for providing the AST and the operational support necessary for the successful completion of the experimental portion of this work. We also wish to thank CTI, Inc., for providing the acoustic transducers and preamplifiers used in the experiment. This work was funded by a contract with the American Petroleum Institute. The authors would like to acknowledge the encouragement and technical review provided by the AST monitoring work group of API's Storage Tank Task Force. Dee Gavora, of API, and Jim Seebold, of Chevron, Inc., were instrumental in promoting the need for AST acoustic leak detection experiments.

REFERENCES

Carter, G. C. 1987. Coherence and Time Delay Estimation. *Proceedings of the IEEE*. 75:2.

Eckert, E. G., and J. W. Maresca, Jr. 1991. Detection of Leaks in the Floor of Aboveground Storage Tanks by Means of a Passive Acoustic Sensing System. *Air and Waste Management Association*. 91.15.5.

Miller, R. K. 1990. Tank Bottom Leak Detection in Above Ground Storage Tanks by Using Acoustic Emission. *Materials Evaluation*. 48(6):822-829.

Nickolaus, C. M. 1988. Acoustic Emission Monitoring of Aboveground Storage Tanks. *Materials Evaluation*. 46:508-512.

APPENDIX B

A PASSIVE-ACOUSTIC METHOD OF DETECTING LEAKS IN THE FLOOR OF AN ABOVEGROUND STORAGE TANK: FIELD TEST RESULTS

Eric G. Eckert and Joseph W. Maresca, Jr.

Vista Research, Inc.
Mountain View, California

A PASSIVE-ACOUSTIC METHOD OF DETECTING LEAKS IN THE FLOOR OF AN ABOVEGROUND STORAGE TANK: FIELD TEST RESULTS

by
Eric G. Eckert and Joseph W. Maresca, Jr.
Vista Research, Inc.
Mountain View, California

ABSTRACT

A leak through a hole in the floor of an AST produces strong impulsive signals provided that the backfill beneath the hole is not saturated with product. Such leaks were successfully detected using an algorithm designed to identify the direct path (leak-to-sensor) signal in the presence of severe multi-path contamination. The distribution of acoustic energy as a function of position on the AST floor was obtained through application of a modified beamforming algorithm to time series of the impulsive leak signal. The leak detection experiments were conducted on a water-filled, 40-ft-diameter AST at a 400-tank oil refinery located in Beaumont, Texas. A trigger threshold of between 20 and 50 times the root-mean-square (rms) noise level was used to initiate data collection by internal and external sensor arrays. Time series of impulsive events were found to be severely contaminated by multi-path signals associated with reflections off the AST shell and air/water interface. In order to distinguish between multi-path signals and the direct-path signal, a double-threshold data quality test was applied to each realization of the leak signal prior to application of the location algorithm. The processing of data contaminated by multi-path signals resulted in the location of virtual images of the leak that were located outside the AST boundary. The combination of high-threshold data acquisition, a double-threshold data quality test, and the modified beamforming algorithm resulted in the successful location of 2.0-mm-diameter leaks into single-bottom and double-bottom backfills, as well as a 3.0-mm-diameter, variable flow-rate leak induced through a leak simulator. A beamforming algorithm was also applied to realizations of the persistent leak signal caused by turbulent flow. The lack of coherence between time series recorded by closely spaced sensors prevented the successful detection of leaks based upon the persistent leak signal.

INTRODUCTION

The successful detection of leaks in the floor of an aboveground storage tank (AST) by passive-acoustic methods requires a detection system capable of accurately estimating the spatial origin of acoustic signals. The manner in which acoustic waves propagate within the confines of an AST and the severe noise environment in which most ASTs are located complicate the design of both the data acquisition system and the processing algorithms that are applied to the measured signals. The characteristics of the acoustic leak signal and ambient noise associated with realistic leaks in the floor of an AST are discussed in Appendix A.

Figure 1 shows a generalized diagram of an acoustic leak detection system. Based upon evidence that the dominant feature of the acoustic leak signal is a large-amplitude, impulsive component that occurs infrequently (Eckert and Maresca, 1991; Miller, 1990; Nickolaus, 1988), data collection is initiated only after a signal is received that exceeds a preset threshold level.

Data are recorded by an array of spatially separated acoustic sensors and consist of either a set of arrival times of the impulsive event or continuous time series of the acoustic leak signal which contain the impulsive event. Once the differential arrival time of the impulsive signal has been measured by the sensor array, a location algorithm is applied in order to estimate the source location (Eckert and Maresca, 1991; Smith and Abel, 1987). If many such events are observed to originate from a localized region of the AST floor, the existence of a leak is inferred.

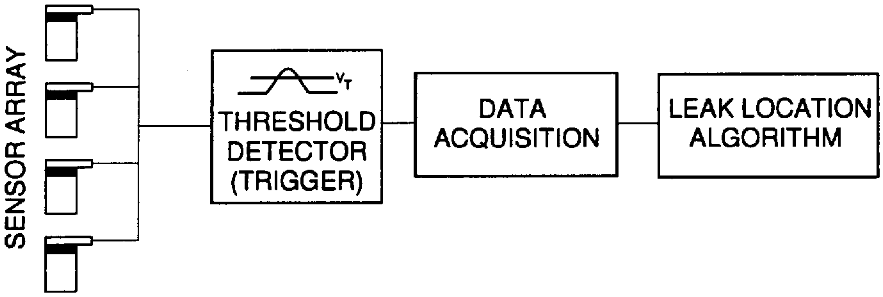

Figure 1. Diagram of a generalized acoustic leak detection system. Data collection is initiated by a signal that exceeds a preset threshold level. The data consist of either impulse arrival times or continuous time series of the leak signal.

Little information has been published concerning the performance of existing AST acoustic leak detection systems (Miller, 1990; Nickolaus, 1988). Expanding upon the results of the signal and noise characterization experiment reported in Appendix A, this work summarizes leak detection field tests conducted on an operational, 40-ft-diameter AST outfitted with realistic leaks. The experiment was completed during May and June 1992 at the Mobil Oil Refinery in Beaumont, Texas.

The primary objective of this work was the development and application of a leak location algorithm consistent with the characteristics of the acoustic leak signal. Although the emphasis of this work was on the impulsive component of the leak signal, the persistent leak signal was also addressed. Leaks into two different backfill types were investigated. Sensor arrays were located both inside the AST and on its exterior walls. The effect of multi-path propagation outlined in Appendix A was considered in the context of leak location.

The results of the AST leak detection experiment may be summarized as follows:

- Leaks into sand and native-soil backfills were successfully located using a high-threshold data collection technique and a modified beamforming detection algorithm.
- Multi-path propagation was perceived by the sensor array as a collection of virtual sources lying outside the AST boundary.
- Data quality tests were required in order to minimize the effects of multi-path propagation and impulsive ambient noise.

- Large amplitude, impulsive leak signals were received equally well by internally-submerged and externally mounted acoustic transducers.
- Attempts to locate AST leaks based upon the persistent component of the acoustic leak signal were unsuccessful.

EXPERIMENT DESIGN

The 40-ft-diameter AST used in the field tests was located at the northern edge of the Mobil-Beaumont refinery. The physical setting in which the AST was situated included many potential sources of ambient acoustic noise: roadways, leaking valves connecting steam pipes to nearby tanks, a steel recycling plant located approximately 1000 ft from the AST, and a nearby dock at which the loading or off-loading of ships frequently took place. In addition to these industrial activities, natural phenomena such as wind, rain, and condensation influenced the acoustic environment in which the experiments were conducted.

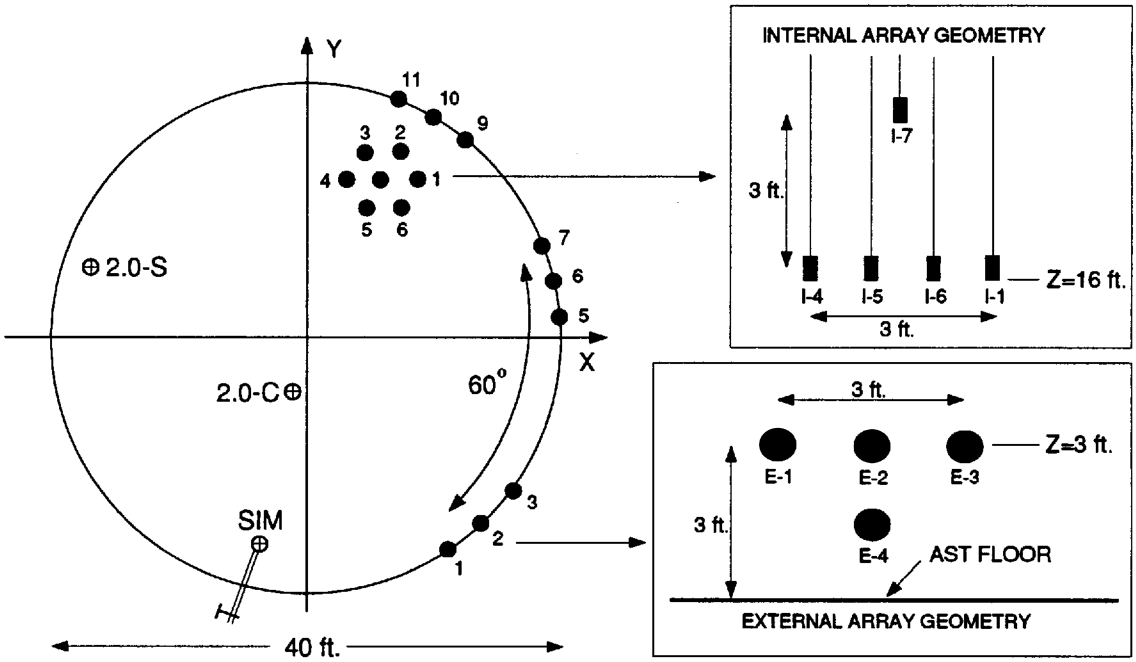

Figure 2. Location of leaks, and geometry of 7-element internal and 12-element external sensor arrays (not to scale).

The AST was of double-bottom construction, with a 6-in. space separating the outer bottom and the "false" or inner bottom. The space between the two bottoms was filled with sand, and the backfill beneath the outer bottom was native soil. Because the AST was being taken out of service, it could be specially configured for the experimental program. The AST had been cleaned and inspected prior to the placement of the holes in the false bottom and the installation of the hardware to control the leaks from these holes.

The water level in the tank was maintained at 25 ft throughout the experimental period. Figure

2 shows the location and diameter of holes used in the leak detection experiments as well as the geometry of the internal and external sensor arrays. Three holes were used to generate the leaks for these experiments: 2.0-mm-diameter holes located near the side (2.0-S) and center (2.0-C) of the AST, and a 3.0-mm-diameter hole that provided flow into a leak simulator (SIM). The backfill beneath each of the three holes is shown in Figure 3. The 2.0-mm-diameter hole near the edge of the AST (2.0-S) drained into a 6-in.-thick sand backfill located between the original and false bottoms of the AST. The design of the double bottom was such that the sand backfill was well drained throughout the experiment. A 1-ft-diameter section of the original bottom was removed beneath the center hole (2.0-C), and the backfill replaced with native soil (a mixture of sand, gravel and clay). The center leaks were designed to reproduce the signal associated with a leak in the floor of a single-bottom AST. The leak simulator, which was welded to the AST floor, consisted of a 1-ft-diameter steel cylinder capped at both ends and fitted with a 3.0-mm-diameter leak hole. The backfill inside the leak simulator was native soil, and the output of the simulator was piped through the AST shell. The flow rate for leaks induced with the simulator was controlled by a valve external to the AST. The devices used to control the on-off status of the leaks and to measure the flow rate are detailed in Appendix A.

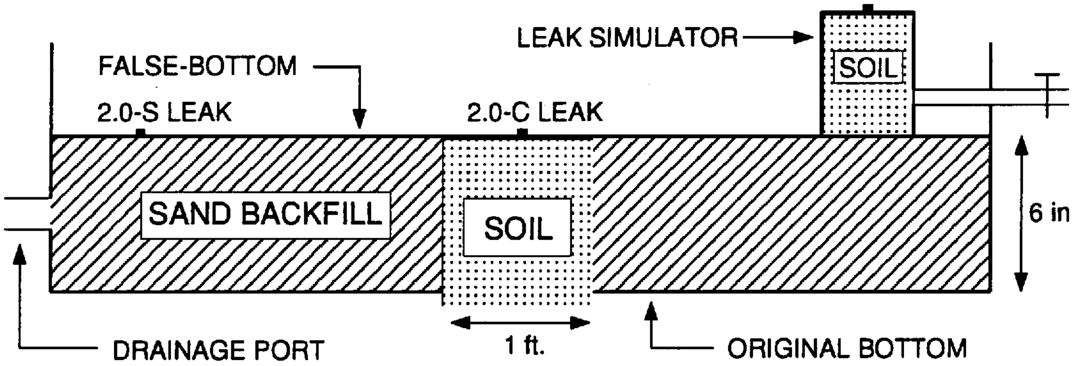

Figure 3. Backfill conditions for 2.0-S, 2.0-C, and Simulated leaks (not to scale). Four drainage ports were open throughout the field tests. Leak simulator flow rate was controlled by a valve external to the AST.

Two sensor arrays were employed in the collection and analysis of the acoustic leak signals. Figure 2 shows the transducer locations for a wide-aperture, 12-element external array and a narrow-aperture, 7-element internally-submerged array. The sensors chosen for the experiment were CTI-30, 30-kHz resonant piezoelectric transducers. While the CTI-30 is primarily designed for high-frequency acoustic emissions applications (due to the strong resonant response near 30 kHz), the transducer is also quite sensitive at lower, audio frequencies (DC-20 kHz). The external array was arranged in three sub-arrays of 4 elements each, located at 0°, 60°, and 120° angular positions on the AST circumference. The element spacing within each sub-array was 1.5 ft. The internal sensor array was deployed down a 3-ft-diameter manway located near the northeast edge of the AST. Elements of the internal array were also spaced approximately 1.5 ft from one another.

A diagram of the data acquisition system used in the the experiments is shown in Figure 4.

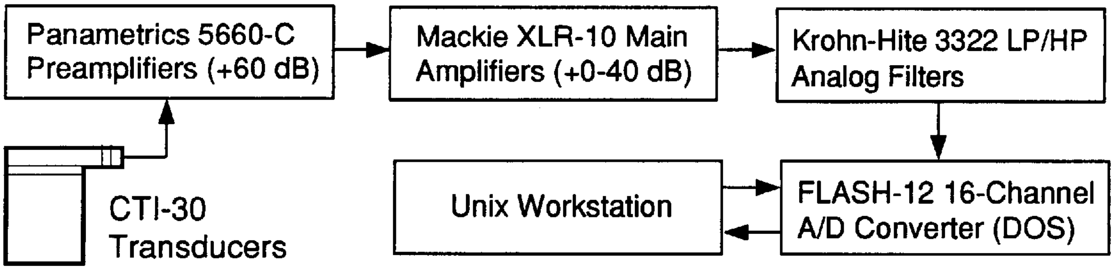

Figure 4. Diagram of the data acquisition system used in the field experiments.

The output of each CTI-30 transducer was amplified by approximately +100 dB in two stages by Panametrics 5660-C preamplifiers and Mackie XLR-10 main amplifiers. The amplified signals were filtered using Krohn-Hite 3322 analog bandpass filters. The analog signals were digitized by a 16-channel STI Flash-12 data acquisition board housed in a DOS micro-computer. Data analysis and the initiation of data collection were controlled by a Unix workstation that was linked to the DOS computer through a local network. The combination of sensors and amplifiers chosen for the experiment resulted in a very low level of system noise. Acquisition of 1-million samples at sampling frequencies up to 62.5 kHz was possible.

DATA

The data collected during the experiments consisted of continuous time series of pressure fluctuations recorded simultaneously by an array of between 6 and 12 acoustic sensors. Such a data set is referred to as a *realization* in this work. The number of realizations processed by the detection algorithm during a given experiment ranged between 50 and 500. The length of the time series recorded by an individual array element was between 1024 points (for measurements of the impulsive leak signal) and 16384 points (for measurements of the persistent leak signal). Sampling frequencies used in the experiments were 62.5 kHz (all impulsive leak signals and some persistent leak signals) and 10.0 kHz (most persistent leak signals). An experiment in which 500 realizations of 16384 points each are collected at a sampling frequency of 10 kHz results in a data set 820 s in duration.

In order to evaluate the capability of the detection system to locate AST leaks based upon the persistent leak signal, data sets were collected in such a way as to minimize the effects of ambient noise. Attempts were made to avoid environmental noise sources (e.g., wind, rain, and condensation) and industrial noise sources (e.g., traffic, nearby factories) through careful choice of the data collection period. Data sets in which a 15 kHz high-pass analog filter was applied to the impulsive leak signal prior to digitization exhibited low levels of contamination by ambient noise. Time series of the persistent leak signal recorded using a 31.25 kHz low-pass filter were severely contaminated by noise at frequencies below 10 kHz, even during experimental periods judged to be relatively quiet. The source mechanisms that give rise to the persistent leak signal and the spectral characteristics of the signal relative to the ambient noise are described in Appendix A. The persistent leak signal is, by definition, assumed to be present during any measurement period, thus, the acquisition of persistent leak signals was not initiated by a trigger event. The total time required for the collection of 50 to 500 realizations of the persistent leak signal was between 30 min and 6 h. Substantial fluctuations in the ambient noise level were observed even during relatively quiet periods. In order to identify realizations of the leak signal that were contaminated by noise fluctuations, a simple data quality test was applied to the persistent leak signal time series prior to application of the detection algorithm. The variance of the received signal within a preset frequency band (typically from 0.5 to 5.0 kHz) was computed for each member of the ensemble of realizations. Realizations for which the deviation of the variance exceeded twice the ensemble standard deviation were assumed to be contaminated by noise and were eliminated from further processing.

TABLE 1 – Summary of data collected during leak detection experiments.

Source	Realizations	Array[1]	f_s (kHz)	Points/Ch.	Time[2](min)
Persistent Leak Signal (non-triggered DAcq)					
2.0-C	500	EA-12	10	16 384	300
2.0-C	500	EA-12	62.5	16 384	300
2.0-C	100	EA-6, IA-7	10	4096	60
2.0-S	500	EA-12	10	16 384	300
2.0-S	500	EA-12	62.5	16 384	300
2.0-S	100	EA-6, IA-7	10	4096	60
Simulator	100	EA-12	62.5	4096	60
Simulator	100	EA-12	10	4096	60
Ambient Noise	150	EA-12	62.5	4096	90
Impulsive Leak Signal (triggered DAcq)					
2.0-C	40	IA-7	62.5	2048	120
2.0-C	200	EA-6, IA-7	62.5	2048	900
2.0-S	400	IA-7	62.5	1024	120
Simulator	400	EA-6, IA-7	62.5	2048	400
Calibration	100	EA-6, IA-7	62.5	2048	60

[1] EA-12 (External, 12-element array), IA-7 (Internal, 7-element array)
EA-6 (External, 6-element subset of EA-12)

[2] Approximate duration of experiment

The procedure used to collect time series of impulsive leak signals is different from that described above in two respects. Because the impulsive signal is not likely to be present during an arbitrary data collection period, a preset threshold signal level is established that must be exceeded by one element of the sensor array prior to the initiation of data collection. Also, since impulsive events are relatively localized in time, the time series acquired are somewhat shorter (1024 to 4096 points) than those used in the persistent leak signal experiments. The low level of persistent ambient noise at frequencies above 10 kHz, combined with the broadband nature of the impulsive leak signal, allowed for measurements to be made during any period that was free of impulsive noise sources (e.g., rain and condensation). Based upon preliminary measurements of acoustic impulses produced by the leak simulator, the trigger threshold was chosen to be within the range $20 \leq V_T/V_n \leq 50$, where V_n was the measured root-mean-square (rms) noise level in the absence of impulses. As with the persistent leak signals, data quality tests must be applied to the impulsive leak signals in order to accurately determine the source location. The nature of these data quality tests is described in a later section of this work. Table 1 presents a summary of the data collected during the leak detection experiments.

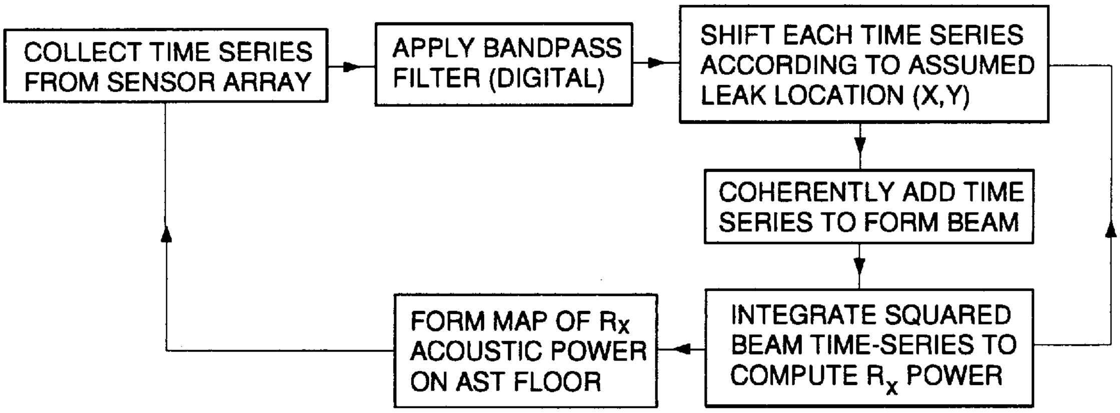

Figure 5. Diagram of beamforming detection algorithm applied to the persistent leak signal. Received (R_x) power is computed as a function of position on the AST floor.

DETECTION OF THE PERSISTENT LEAK SIGNAL

If the persistent leak signal is sufficiently strong in comparison to ambient noise, and if the signal received by each sensor is composed mainly of energy propagated along a single path, then a beamforming detection algorithm may be used to locate the source of the leak (Eckert and Maresca, 1991; Van Veen and Buckley, 1988). Figure 5 shows a diagram of the beamforming detection algorithm as applied to the persistent leak signal. The main assumptions underlying the algorithm are: (a) the gain in received power resulting from the coherent addition of time series of the leak signal exceeds the gain expected from the addition of uncorrelated noise by a factor of n, where n is the number of array elements; (b) an array of acoustic sensors may be positioned in such a way as to accurately detect the position of a localized source of coherent signals; and (c) the ability to detect a weak source improves as more realizations of the signal are processed. The directional sensitivity of the array is adjusted by shifting the time series relative to one another prior to coherently adding the individual signals. By dividing the AST floor into a large number of grid points (typically $\sim$ 5000), the hypothesis that a leak exists at each grid location may be tested. The output of the beamforming algorithm applied to a single realization of the leak signal is a map of received acoustic power as a function of position on the AST floor. Additional sensitivity to the presense of a leak may be attained by processing many realizations and computing the deviation of the received power at each grid point from an average power level computed over the entire tank floor, and over all realizations. This type of acoustic map is referred to as the signal-to-noise (SNR) power. The ability of the beamforming algorithm to correctly identify the source location of coherent signals was tested through the use of simulated time series in which a coherent signal was partially masked by noise. Figure 6 shows the SNR power computed from 10 realizations of simulated data in which the single-transducer SNR within the 1- to 5-kHz band was 1.1. Propagation of the simulated leak signal was confined to a single path from source to sensor (i.e., no multi-path). The length of the time series was 4096 points and the sampling frequency was set to 10 kHz. The simulated time series were computed for each element of the 12-element external array used in the AST experiments; the beamforming algorithm was applied to a 73x73-point grid centered on the AST floor. The estimated location of maximum SNR power agrees with the location of the simulated source to within the grid spacing. The simulation results have been scaled such that the maximum SNR power is equal to 100.

Investigations of the persistent leak signal from the perspective of source location were conducted as part of the experimental program. Figure 7 shows time series of the persistent acoustic leak signal recorded by two external CTI-30 transducers (E-5 and E-6) in the presence of a leak through the 2.0-mm-diameter hole (2.0-S) into the false bottom backfill. A time series of ambient noise (no leak) is shown for reference. The separation between the sensors is 1.5 ft. In order to estimate the source location of the leak, the differential arrival time of the leak signal at spatially separated sensor locations must be obtained. The complex coherence function computed between two time series provides a measure of the accuracy with which the differential arrival time may be estimated (Carter, 1987). The amplitude of the coherence function computed between the time series of Figure 7 is shown in Figure 8. Frequencies for which the coherence amplitude lies above the 95% level of statistical significance indicate that the differential arrival time may be accurately estimated at the particular frequency. It should be noted that at frequencies greater than ~ 500 Hz (below which the ambient noise is strongly correlated), no statistically significant coherence is observed between time series of the persistent leak signal. As noted in Appendix A, this observed lack of coherence is caused by (a) high levels of ambient noise at frequencies below ~ 10 kHz and (b) multi-path propagation (i.e., reflection signals) within the AST. Though a single realization of the persistent leak signal does not provide information of sufficient quality to locate the leak (due to low coherence), a beamforming detection algorithm applied to the entire 12-element array and averaged over many realizations may be used to enhance the leak signal relative to ambient noise.

Figure 9 shows the SNR power as a function of position resulting from the application of the beamforming algorithm to 500 realizations of persistent leak signal data. The data sets were recorded during a 6-h period when the 2.0-S leak was active and the ambient noise level was

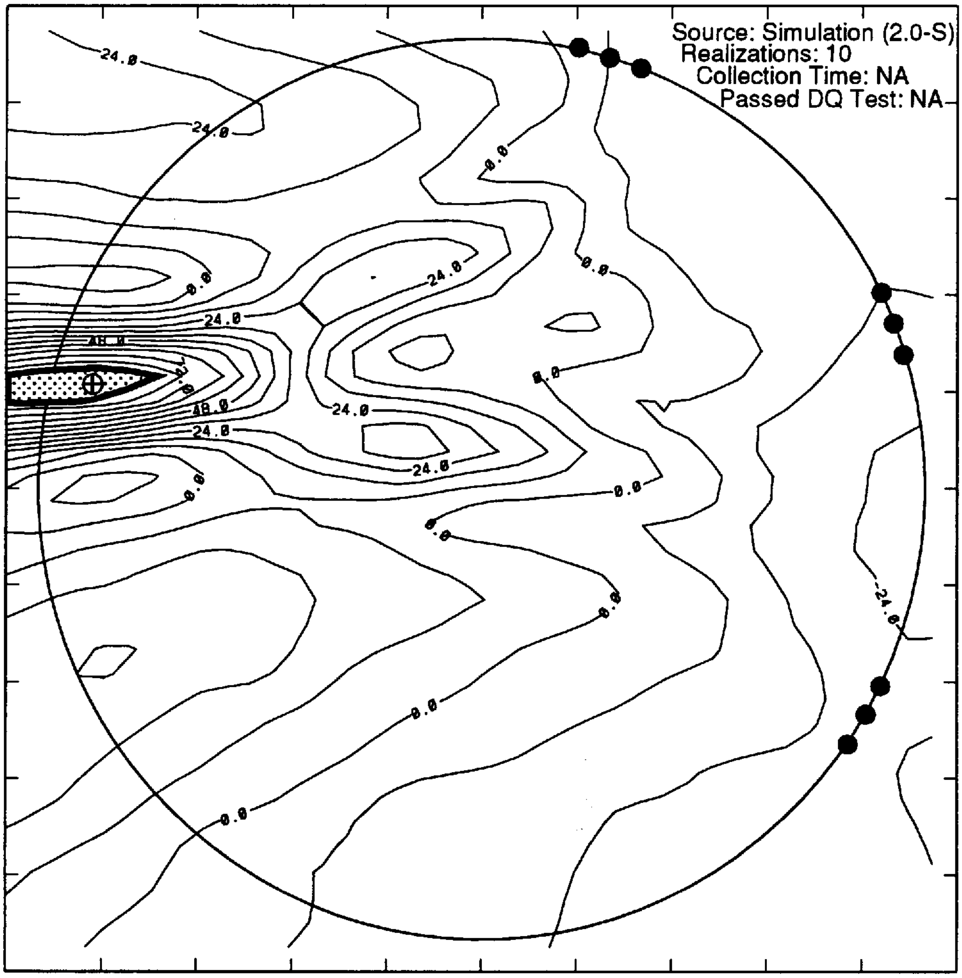

Figure 6. Map of SNR power as a function of position on the AST floor. Source is 10 realizations of simulated leak signals within 1- to 5-kHz band. Individual sensor SNR of 1.1 is achieved through addition of noise. Bold contour encloses region for which received SNR power is within 10% of maximum. Simulated source location (2.0-S) and computed maximum power location lie on same grid point (indicated by marker).

judged to be low. Approximately 7 min of data were processed to generate the map of Figure 9. The beamforming algorithm was applied to a 73x73-point grid; each time series was bandpass-filtered between 1.0 and 5.0 kHz prior to the formation of the beam. The most striking feature of Figure 9 is that even after 500 realizations of the persistent leak signal have been processed, there is no indication that the leak has been detected above the ambient noise level. Because of the extremely low coherence between time series recorded by closely spaced sensors, there appears to be little hope for the successful detection of small AST leaks based upon the persistent leak signal. With regard to passive-acoustic leak detection, the persistent leak signal must be viewed as a source of noise.

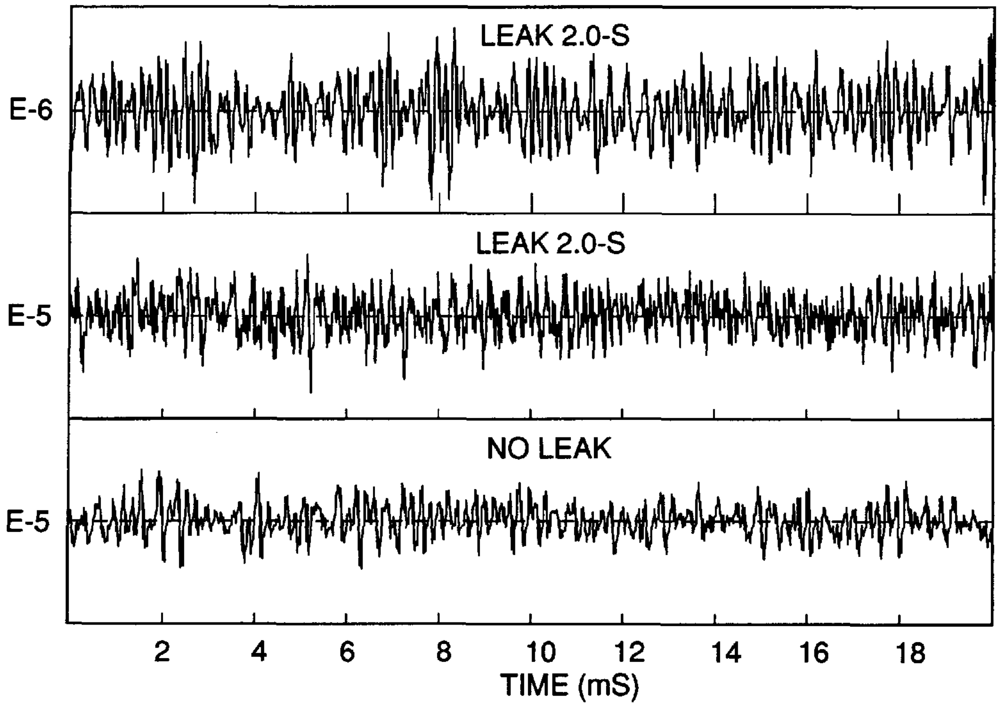

Figure 7. Time series of the persistent leak signal produced the the 2.0-S leak. A time series recorded under no-leak conditions is shown for reference.

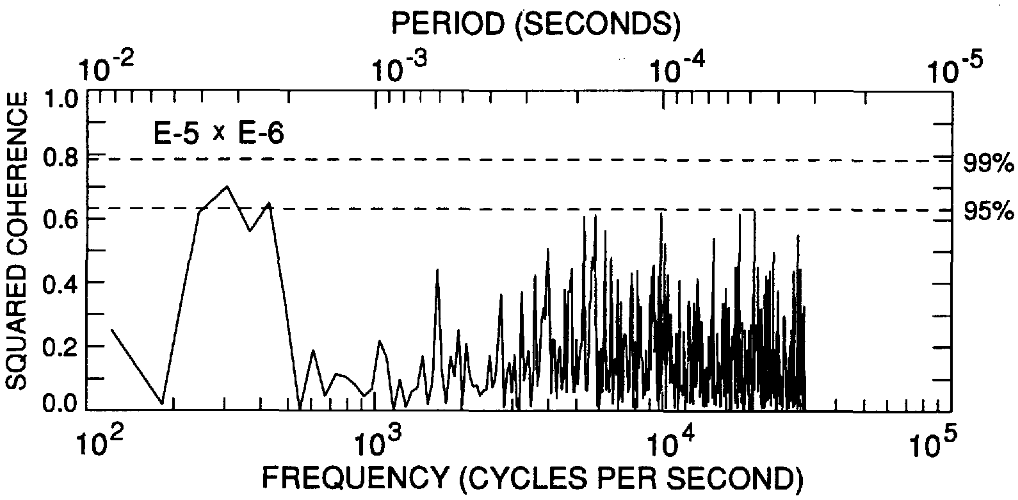

Figure 8. Coherence amplitude computed between time series of the persistent leak signal recorded by external-array elements E-5 and E-6. Sample frequency is 62.5 kHz; sensor separation is 1.5 ft.

DETECTION OF THE IMPULSIVE LEAK SIGNAL

Figure 10 shows time series of the impulsive leak signal produced by a leak through the 2.0-mm-diameter hole in the false bottom and into the sand backfill. The time series were recorded by internal sensors (I-2 and I-5) separated from one another by 1.5 ft. Simulations of the propagation of impulsive signals within the AST geometry suggest that all of the impulses present in Figure 10 are caused by the emission of a single event from the leak location. Trailing the direct-path signal, a series of multi-path reflection signals are received. The

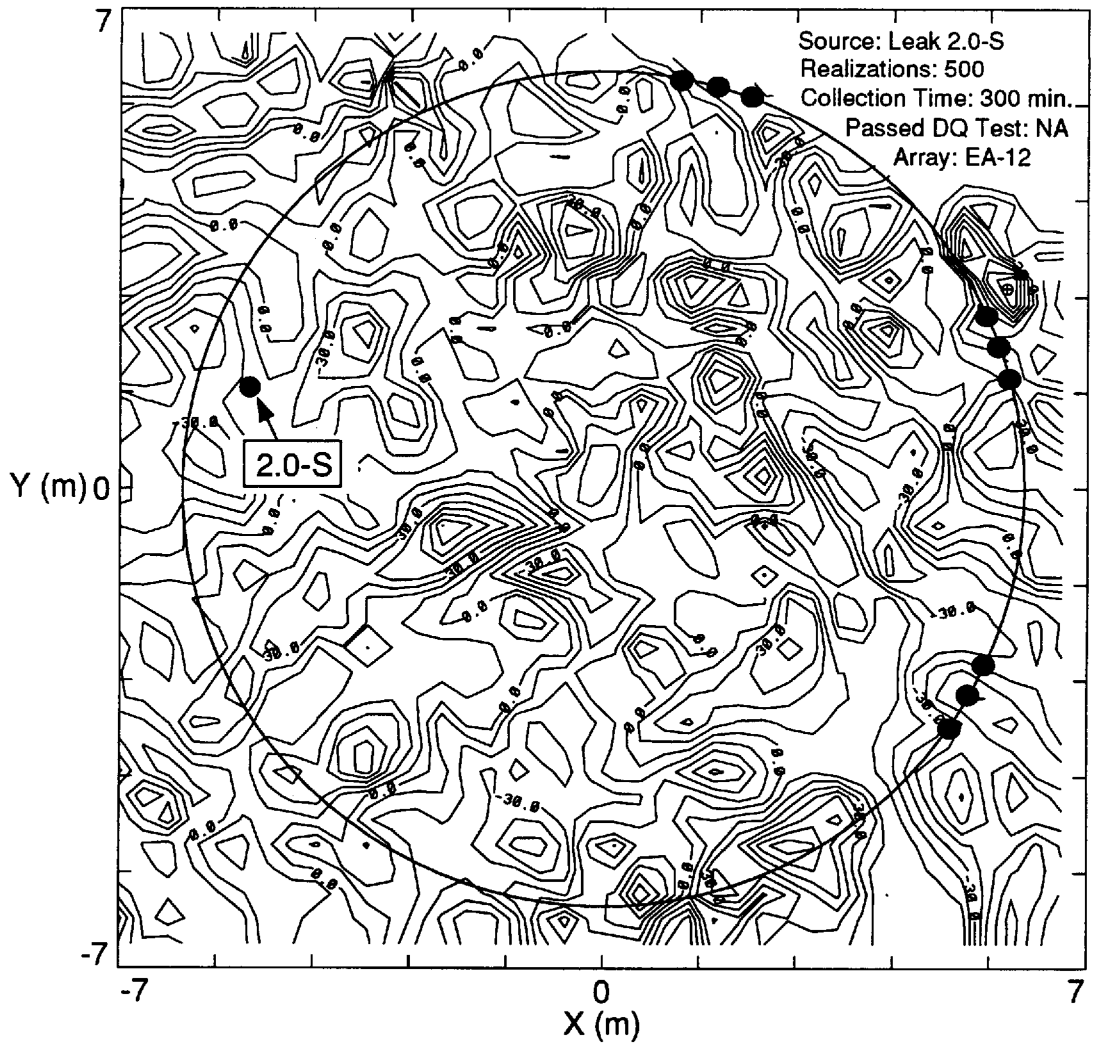

Figure 9. Map of SNR power as a function of position on the AST floor. Beamforming algorithm was applied to 500 realizations of the 2.0-S persistent leak signal. Position of leak is indicated by marker.

amplitude of the reflection signals relative to the direct-path signal depends upon the location of both source and sensor, and on the diameter of the AST (Appendix A). Multi-path signals recorded during the field tests were frequently observed to exceed the direct-path signal in amplitude. In addition, the duration of the reverberation field was long (~ 2D/c). Acoustic leak detection systems that do not recognize the importance of multi-path propagation may encounter problems in locating impulsive sources within the reverberant AST environment.

Consider the case of a simple acoustic leak detection system that measures only the arrival time of impulsive events at an array of sensors and estimates the source location by application of a triangulation algorithm (Eckert and Maresca, 1991; Smith and Abel, 1987). If such a system operates in a reverberant environment, many of the measured arrival times will be contaminated by multi-path signals. The effect of such contamination on the ensemble of location estimates computed over the course of a leak detection test will depend upon the ability of the location algorithm to recognize when multi-path signals are received. Without the collection of time

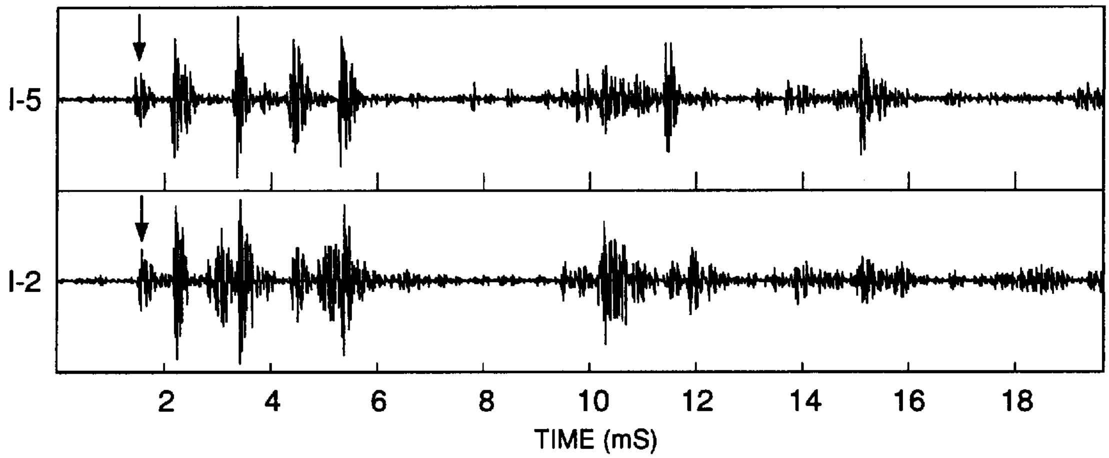

Figure 10. Time series of impulsive leak signal produced by a 2.0-mm-diameter leak into the false-bottom (sand) backfill. Sensors are internal CTI-30s (I-2 and I-5) separated by 1.5 ft; leak-to-sensor distance is ~ 30 ft. Direct-path impulse is indicated by arrows.

series, this recognition involves a consistency check on the source location of each impulsive event among several combinations of array elements. If the multi-path contamination is severe, this type of system must discard a great deal of information associated with the leak in order to process only those sets of impulse arrival times in which the direct-path is represented. The classical beamforming algorithm described in the previous section is similarly affected by multi-path propagation. From the perspective of a beamforming array, multi-path signals appear as a collection of virtual sources whose origins do not coincide with that of the true leak. Thus, instead of detecting the leak against a small ambient noise level, the leak location must be identified against a large number of apparent sources caused by multi-path signals. Figure 11, in which direct-path and single-reflection rays are propagated from a source to internal and external sensors, illustrates the formation of virtual images of the leak that lie outside of the AST boundary. Virtual images associated with the 2.0-S source and IA-7 array are shown in Figure 12. This figure also demonstrates the manner in which acoustic energy is focused by the AST wall, creating multi-path signals that frequently exceed the direct-path signal in amplitude. A modified version of the beamforming algorithm was combined with a set of data quality tests in order to correctly interpret the impulsive leak signal.

Figure 13 shows a diagram of the modified beamforming algorithm as applied to the impulsive leak signal. Whereas the original algorithm was designed to achieve a gain in signal strength over ambient noise by coherently adding time series of pressure fluctuations, the modified algorithm forms a beam through the addition of time series of received power. This approach is required due to the frequency content of the impulsive time series. The low level of ambient noise associated with time series of high-frequency, impulsive leak signals is gained at the expense of coherence. The coherence between time series of an individual impulse is extremely low due to (1) the manner in which the resonant sensors respond to impulsive input and (2) the relatively large separation between sensors (in comparison to the signal wavelength). Similarity is maintained, however, within the envelope of the received signal.

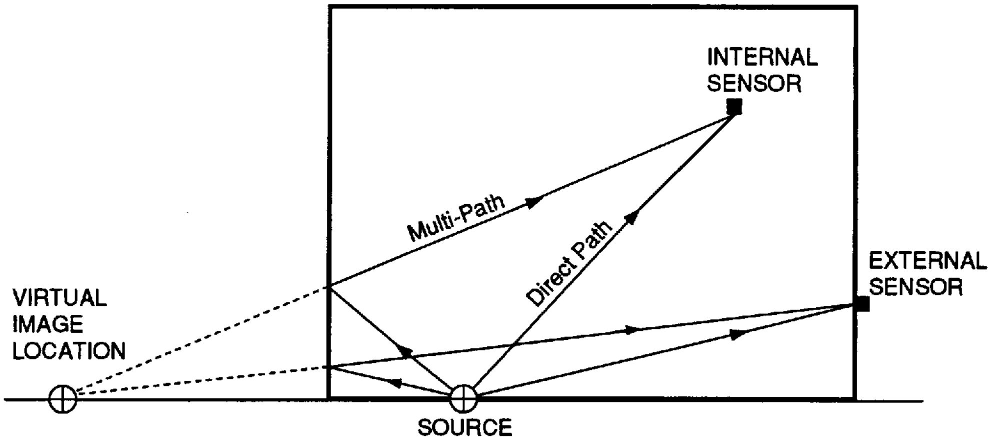

Figure 11. Diagram of direct-path and single-reflection acoustic rays propagated from a source to internal and external sensors. The projection of the reflection rays onto the z=0 plane (AST floor) defines the location of virtual images associated with the source.

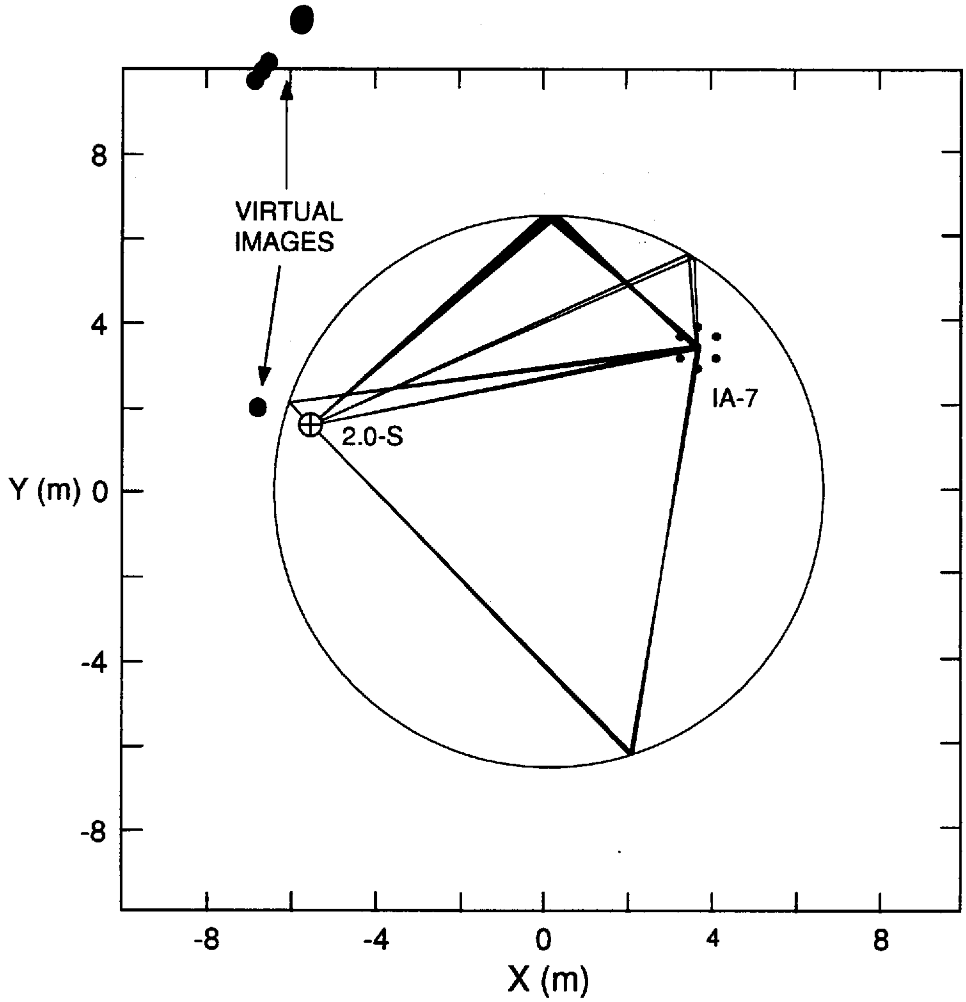

Figure 12. Results of a ray-tracing simulation applied to the 2.0-S source and IA-7 sensor array. The scale is similar to that used in Figure 19, in which the strong virtual source in the upper left-hand corner was imaged from actual data.

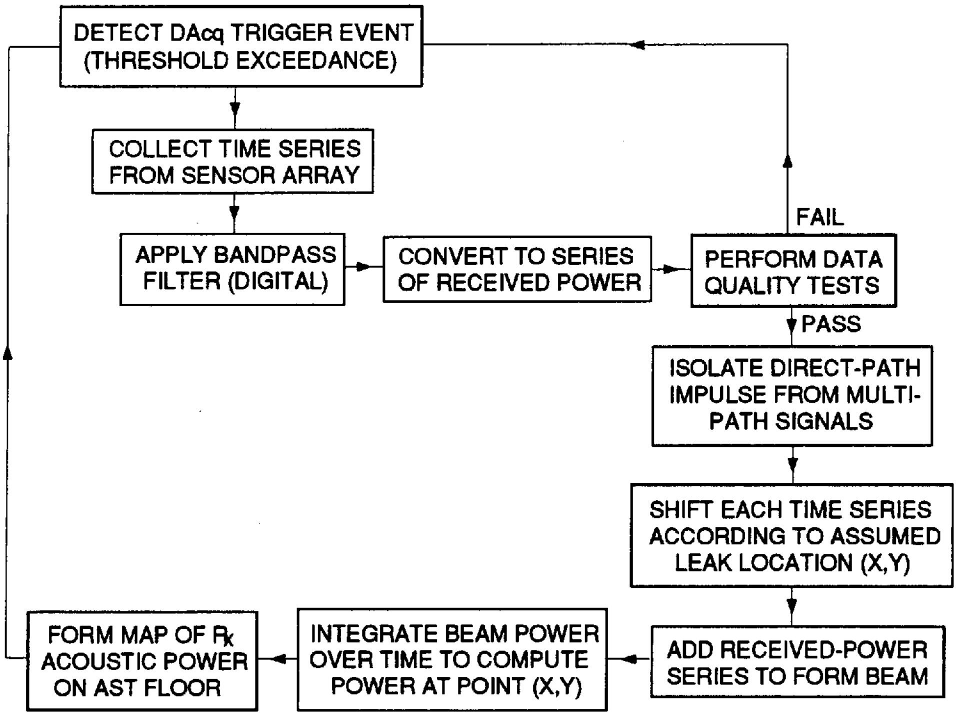

Figure 13. Diagram of modified beamforming detection algorithm applied to impulsive leak signal.

The received power measures the envelope of the signal as a function of time, and so provides the best input to the detection algorithm. Data quality tests are applied to the impulsive leak signals in order to determine that (a) impulses processed by the detection algorithm correspond to signals propagated along the direct path from source to sensor and (b) that the origin of the impulse is below the sensor array (i.e., from the AST floor).

Figure 14 shows time series of impulsive leak signals that demonstrate the application of the first data quality test. In both time series of Figure 14, the time at which the threshold exceedance occurred is known. Figure 14a is an example of an event in which a multi-path signal initiates the collection of data. An array of sensors responding to this event would locate the multi-path source rather than the true leak. In order to recognize that a multi-path signal has provided the trigger event, a secondary threshold is applied to the recorded time series. The level of the secondary threshold must be set far enough below the primary threshold so that impulses which precede the trigger event are detected, but high enough above it to be unaffected by fluctuations in ambient noise. Through the analysis of many time series such as those of Figure 14, the level of the secondary threshold was empirically established within the range $0.1 \leq V_{T2}/V_{T1} \leq 0.5$, where V_{T1} and V_{T2} represent the primary and secondary threshold levels, respectively. For time series in which the trigger location is known (such as those of Figure 14), a narrow ($\sim$ 0.5-1.0 ms) pulse window is centered on the trigger event. The width of the pulse window is related to the ringing response of the CTI-30 transducer to an impulsive signal. The secondary threshold is applied to a length τ of the time series preceding the pulse

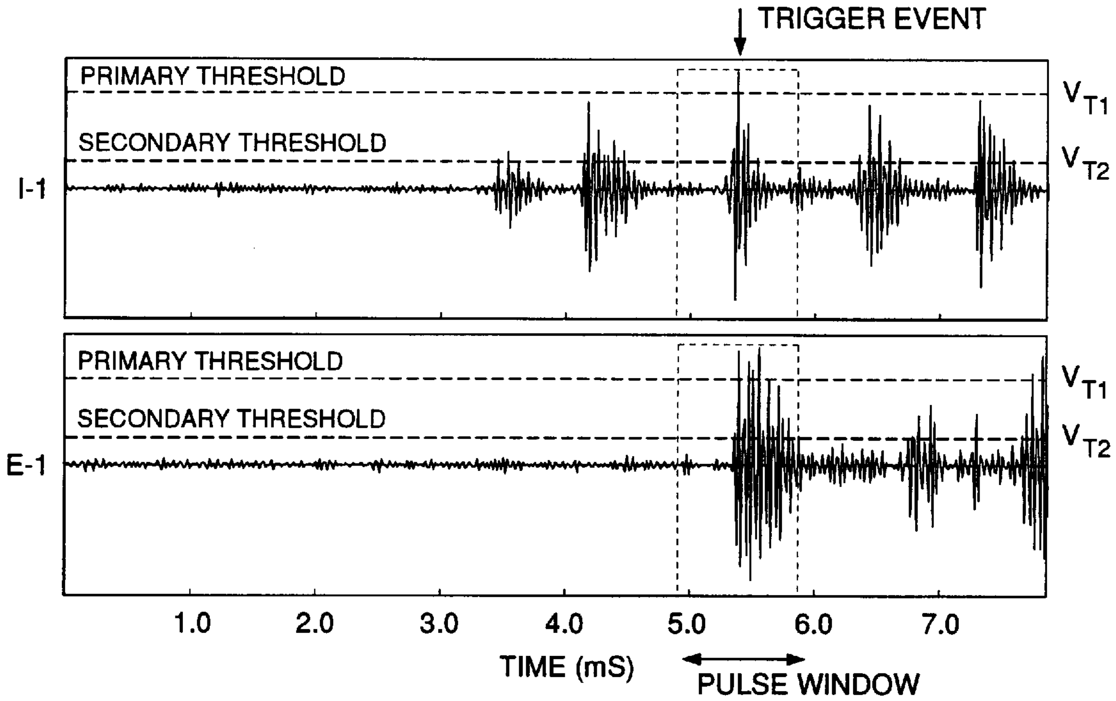

Figure 14. Time series of impulsive leak signals recorded by (a) internal sensor (I-1) with 2.0-S leak active and (b) external sensor (E-1) with leak simulator active. Both signals acted as triggers for data acquisition. Primary threshold for data acquisition and secondary threshold used in data quality test are indicated by dashed lines. Pulse window centered on trigger impulse is also shown.

window. The value of τ was typically chosen to be $\sim$ D/c (8 ms). If any portion of the time series is observed to exceed the secondary threshold during this period, the trigger event is associated with multi-path propagation, and the data quality test fails. Figure 14b shows an example of a time series that passes the secondary-threshold data quality test. Prior to the pulse window containing the trigger event, no signals exceed the secondary threshold. Thus, the trigger event is assumed to represent the direct-path propagation from leak to sensor. The data acquisition system used in the experiments allowed only one channel to act as the trigger. For this reason, the time at which large-amplitude impulses arrive at the remaining sensor locations is not directly measured. In order to apply the secondary threshold test to the non-trigger time series, the pulse window must be adjusted according to the diameter of the AST and the relative positions of the sensors. Figure 15 shows time series in which the pulse windows for three non-trigger time series are indicated. The non-trigger pulse windows represent the *expected* arrival times of the trigger impulse at the remaining array elements, assuming that the signal originated from any location on the AST floor. Once the pulse windows are established for each element of the sensor array, the secondary threshold test can be applied to the entire array. The portion of a time series recorded after the passage of the pulse window is assumed to be composed entirely of multi-path signals. In order to minimize the effects of these signals on the subsequent application of the beamforming location algorithm, the signal is set to zero outside the pulse window. The result of this operation, along with the conversion of the time

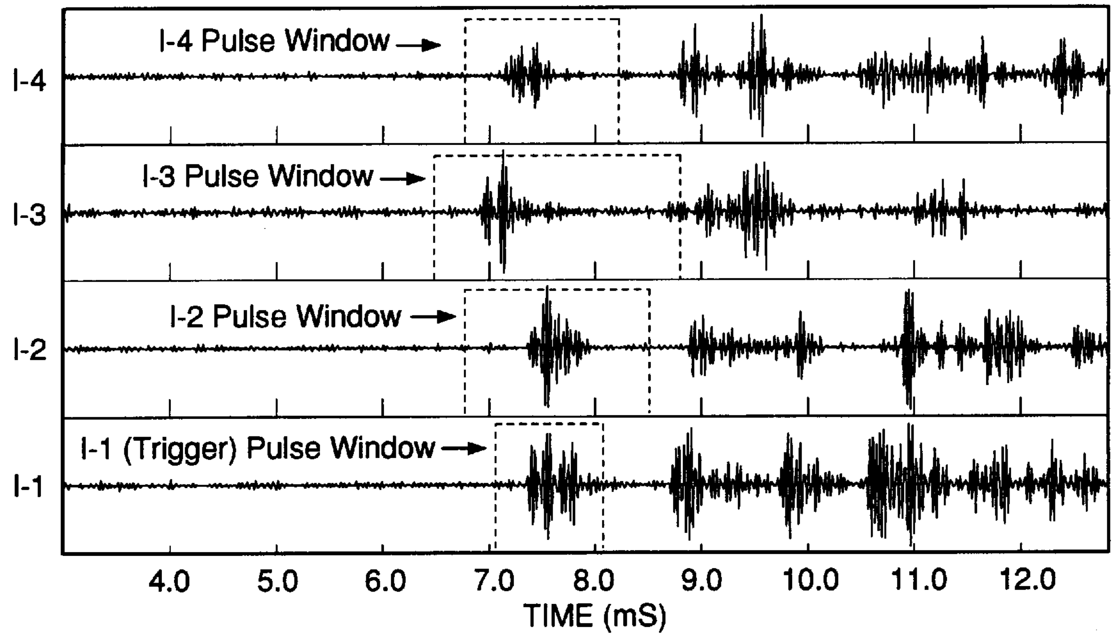

Figure 15. Time series of 2.0-S acoustic leak signals recorded by a narrow-aperture internal array. Dashed windows for sensors I-2, I-3, and I-4 indicate expected arrival time of I-1 impulse based upon array geometry and AST diameter.

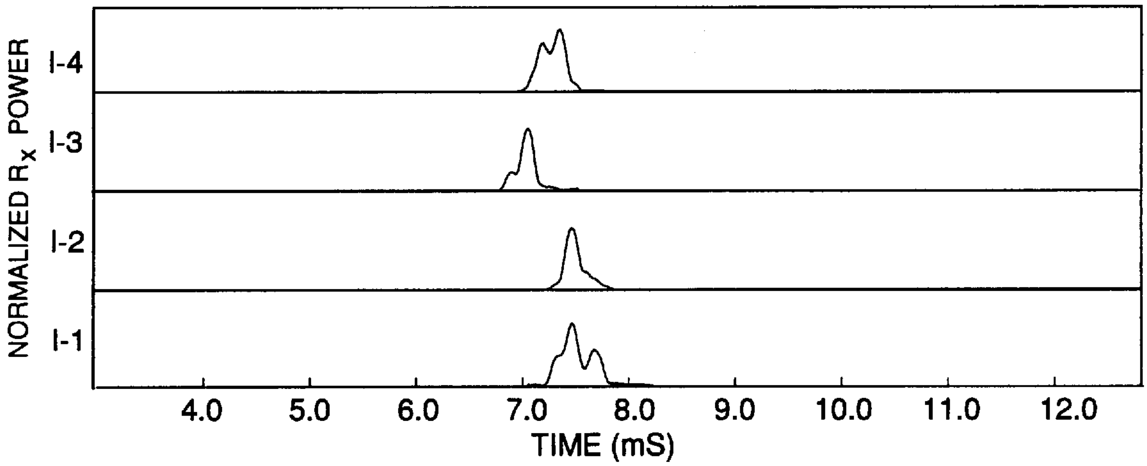

Figure 16. Time series of normalized received power corresponding to data of Figure 15. Multi-path signals lying outside of the direct-path pulse-window are eliminated prior to application of the detection algorithm.

series to received power, is shown in Figure 16. The source location estimate is obtained by shifting data such as that of Figure 16 in time according to a grid of assumed leak locations, and measuring the received power as a function of position on the AST floor.

A second data quality test is required in order to reject impulsive condensation noise that occurs at the air-product interface of an AST. Figure 17 shows time series of a condensation drip recorded by a pair of internal sensors separated vertically by 3 ft. The dashed window within the time series for element I-7 indicates the *expected* arrival time of the I-5 trigger impulse had the impulse been emitted from the AST floor. A threshold test applied to the

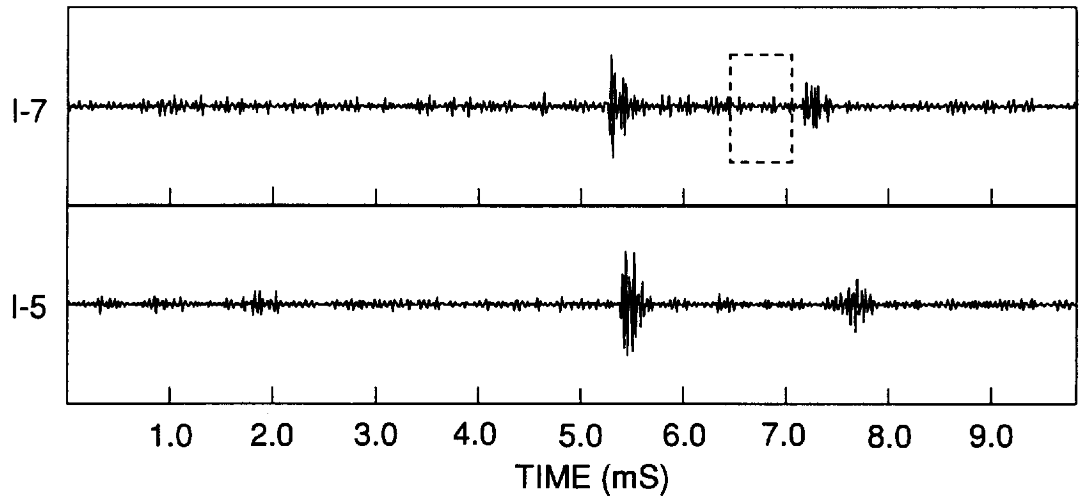

Figure 17. Condensation impulse recorded by two members of the narrow-aperture internal array (I-5 and I-7). Vertical separation between I-5 and I-7 is 3 ft. Expected arrival time of impulse originating from AST floor at the I-7 sensor location is indicated by the dashed window. Strong reflection from the AST shell (multi-path) is also recorded.

portion of the time series preceding this window must be passed in order for the event to qualify as having originated from the AST floor.

RESULTS

As a calibration test, impulsive signals produced by breaking a thin pencil lead against the AST shell were recorded and processed using the modified beamforming algorithm. The calibration signal was generated near the E-8 external sensor location. The separation between the source of the signal and the internal array was approximately 20 ft. Figure 18 shows a map of the SNR power measured from an ensemble of 10 calibration impulses. The predicted and actual source locations differ by less than the grid spacing used to generate the map (1.4 ft).

Figure 19 shows a map of the SNR power computed from an ensemble of 170 realizations of the 2.0-S leak (sand backfill) recorded by a 7-element, narrow-aperture internal array. The primary threshold, V_{T1}, used to collect the data was set at about 25 times the rms noise level; the total time of the experiment was 50 min. The thick contour in the upper left corner of Figure 19 encloses that portion of the z=0 plane (AST floor) for which the SNR power is within 10% of the maximum. The secondary threshold, V_{T2}, was set at a level equal to that of the primary threshold (the threshold used to initiate data acquisition); this data set could thus be processed in such a way as to include impulsive events associated with multi-path propagation. Of the 170 events collected, 168 were used to generate the SNR power map. This map indicates that the location of the acoustic source is outside the AST. A ray-tracing simulation was developed and applied to the 2.0-S source and IA-7 sensor array in order to predict the image location of multi-path signals caused by secondary reflections from the AST

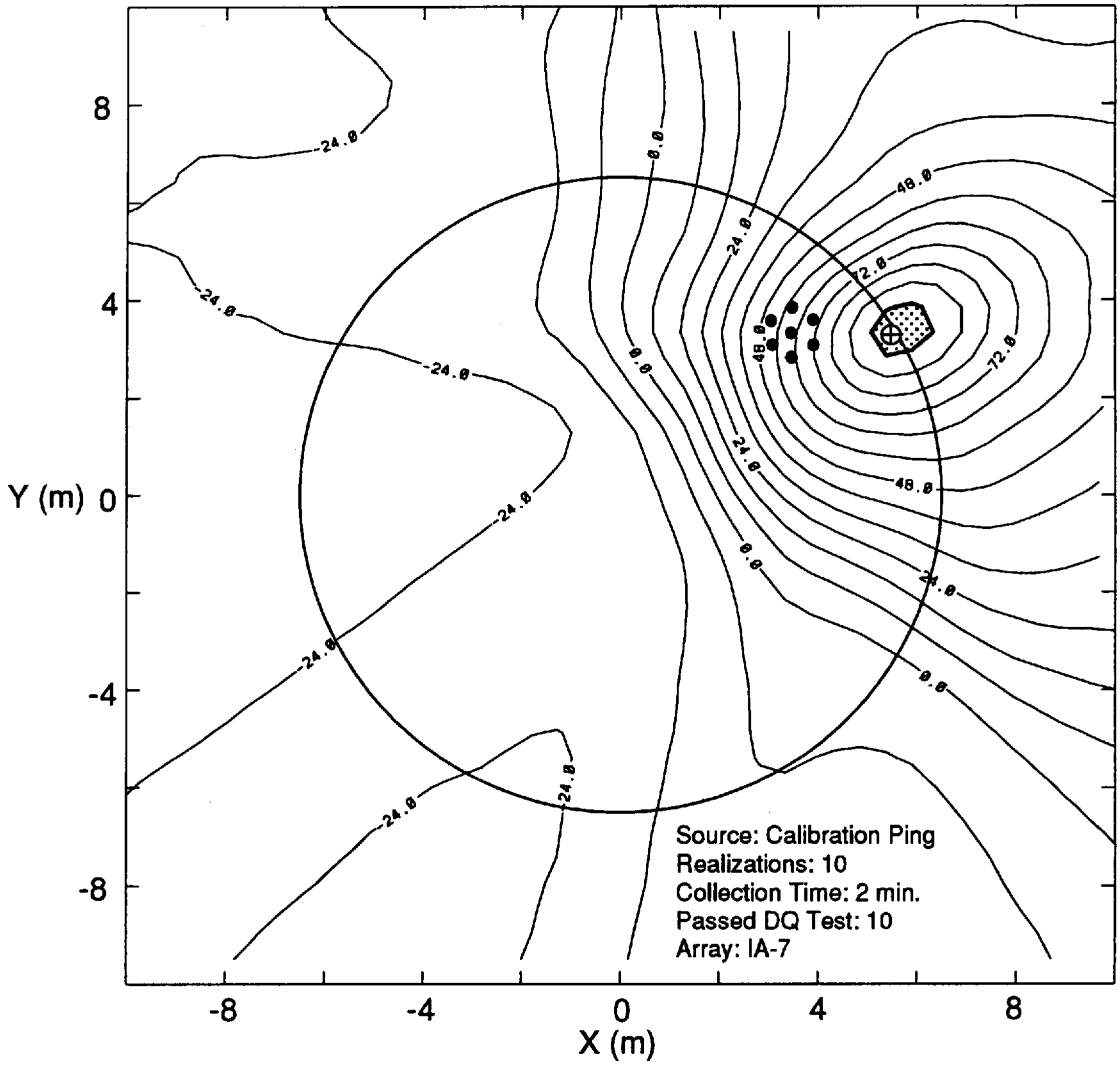

Figure 18. Map of SNR power as a function of position on the AST floor. Modified beamforming algorithm was applied to 10 realizations of an impulsive calibration signal. Bold contour encloses region for which received SNR power is within 10% of the maximum. Source location estimate (maximum received power) is indicated by marker.

shell. The predicted image location of the dominant multi-path signal and the strength of this signal relative to the direct-path signal are consistent with the source location shown in Figure 19 (see Figure 12). The propagation path between source and the sensor corresponding to the strong multi-path image is also shown. Experimental data and ray-tracing simulations suggest that the situation illustrated in Figure 19 (i.e., the presence of strong multi-path signals) is not uncommon (Appendix A). Unless each realization of the impulsive leak signal is tested for multi-path contamination, the leak detection system may locate virtual images of the leak lying outside of the AST boundary rather than the leak itself.

Figure 20 shows a map of SNR power computed from the same data set as that used in Figure 19, wherein the direct-path signal has been isolated and the data then processed. In this case the secondary threshold for the multi-path data quality test was set to 10% of the primary threshold level. Of 170 realizations, only 20 passed the restrictive data quality test. By only

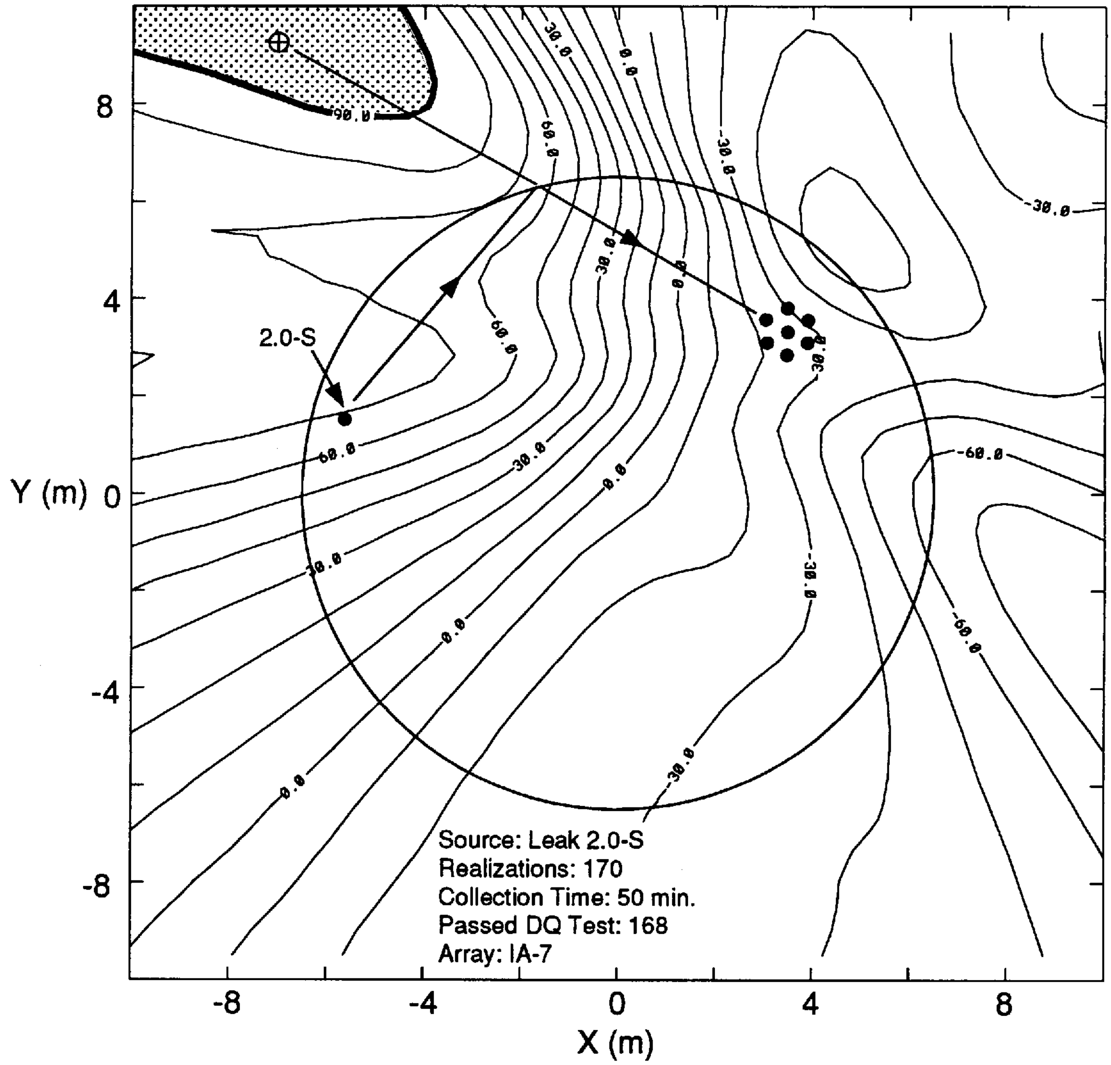

Figure 19. Map of SNR power as a function of position on the AST floor. Modified beamforming algorithm was applied to 170 realizations of the impulsive leak signal produced by leak 2.0-S. Bold contour encloses region for which received SNR power is within 10% of the maximum. Maximum power location is indicated by marker. Propagation path and image location for dominant reflection signal is also shown.

processing the 20 data realizations for which the received impulse is associated with the direct-path signal, the 2.0-mm-diameter side leak is successfully located. The 6-ft difference between the predicted and actual leak locations is most likely caused by uncertainties in the locations of the array elements and by the presence of a relatively strong virtual source caused by reflections of the primary signal off the AST shell immediately behind the leak. Within the time series, the direct-path signal and the first reflection signal are closely spaced (due to the proximity of the 2.0-S leak to the AST wall), and so the process of minimizing the multi-path signal outlined in the previous section is incomplete.

Figure 21 shows a map of SNR power when the leak is produced by the simulator. The map was computed from 40 realizations of data collected during a 40-min period in which the leak simulator was active. The leak flow rate during this experiment was set at 2 gal/h. In this

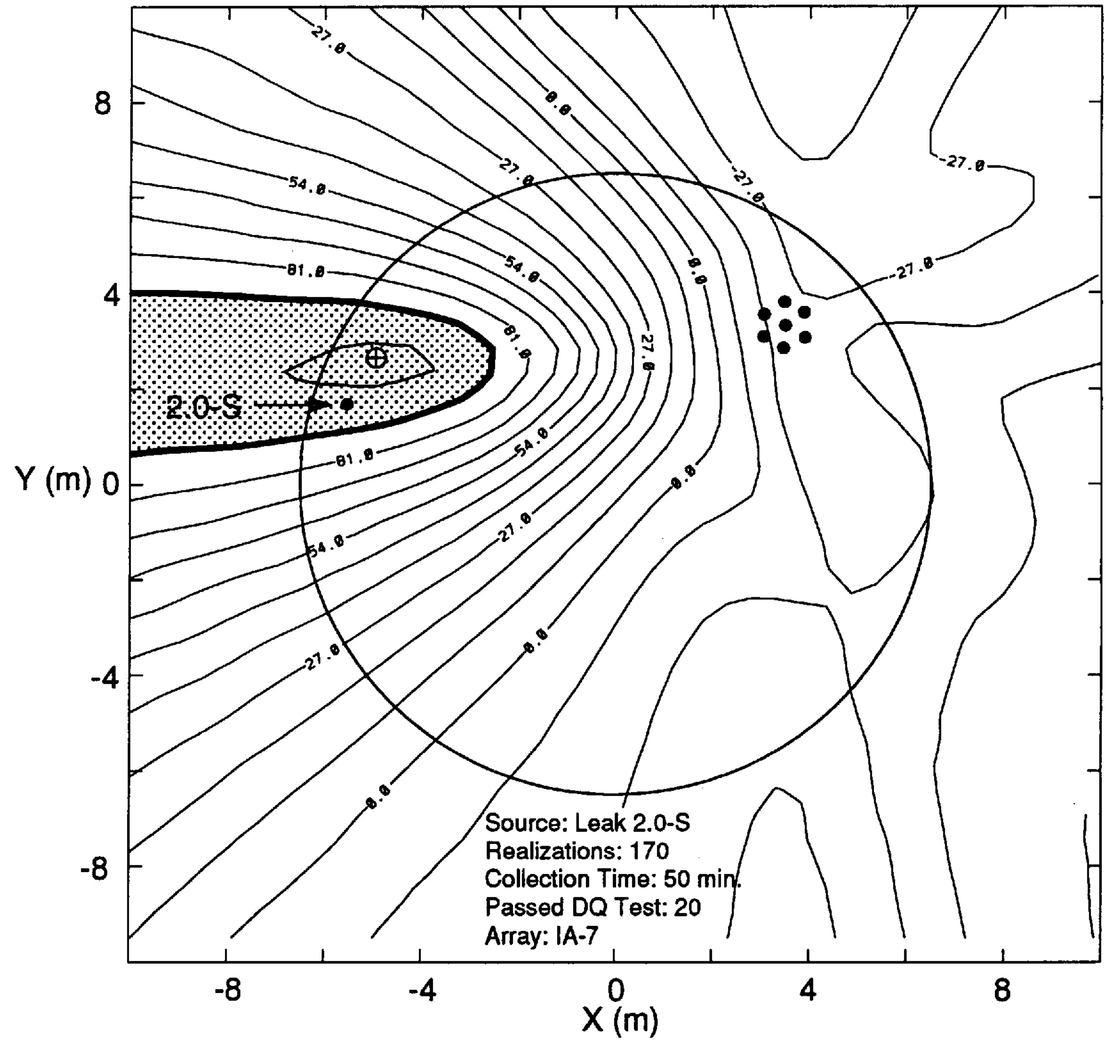

Figure 20. Map of SNR power as a function of position on the AST floor. Modified beamforming algorithm was applied to same data set as Figure 19 (170 realizations of leak 2.0-S). Bold contour encloses region for which received SNR power is within 10% of the maximum. Maximum power location is indicated by marker. Secondary threshold is set to exclude multi-path signals.

instance, the secondary threshold was set to 50% of the primary level. Of the original 40 realizations, 25 were identified by the data quality test as impulses representing the direct-path signal. The sensor array used during this experiment consisted of 6 elements arranged to cover a 120° aperture on the external AST shell. The predicted and actual leak locations agree to within the grid spacing (1.4 ft). Notice that while the source location has been accurately predicted, a second source nearly equal in strength is visible in the lower right corner of the plot. This is a consequence of the less restrictive secondary threshold (i.e., 50% of the primary threshold) used in the separation of direct-path from multi-path signals. A ray tracing simulation shows that this virtual image is consistent with the reception of strong multi-path reflection signals in two of the array elements (E-5 and E-7). In this instance, the multi-path contamination did not degrade the source detection and location.

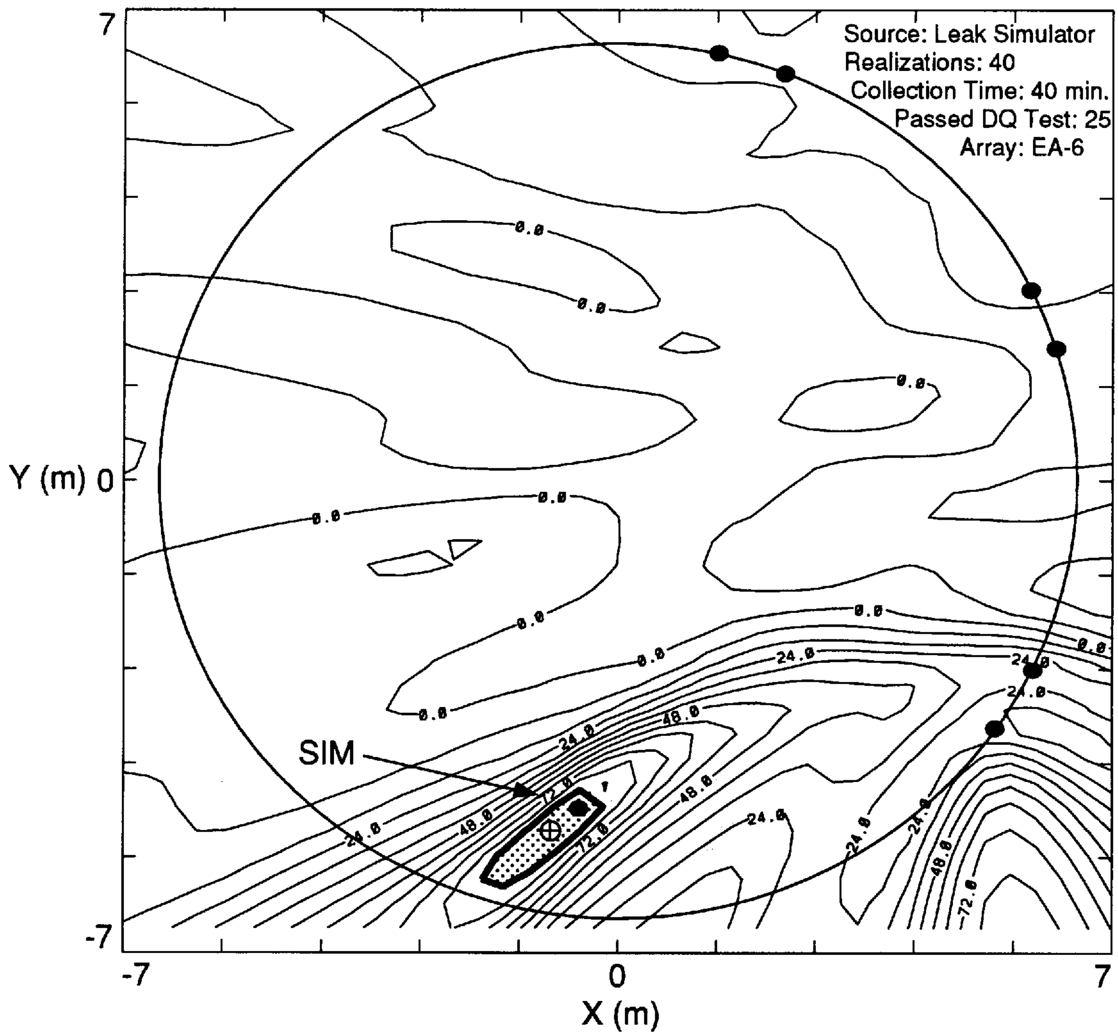

Figure 21. Map of SNR power as a function of position on the AST floor. Modified beamforming algorithm was applied to 40 realizations of acoustic leak signals produced by leak simulator (SIM). Bold contour encloses region for which received SNR power is within 10% of the maximum. Maximum power location is indicated by marker. Multi-path image is visible in lower left portion of map.

Finally, Figure 22 shows a map of the SNR power computed from 100 realizations of data collected during a 150-minute period in which the 2.0-C leak through a single bottom (soil backfill) was active. The secondary threshold used to process these data was set to 10% of the primary value. Of the original 100 realizations, 25 passed the multi-path data quality test. The 6-element, narrow-aperture internal array was able to locate the leak to within 2 ft of the actual position. The locations of the source and sensors are such that the virtual images of reflection signals lie well outside of the AST boundary, and so only the true leak is imaged.

CONCLUSIONS

The acoustic leak detection experiments performed on the 40-ft-diameter AST yielded several

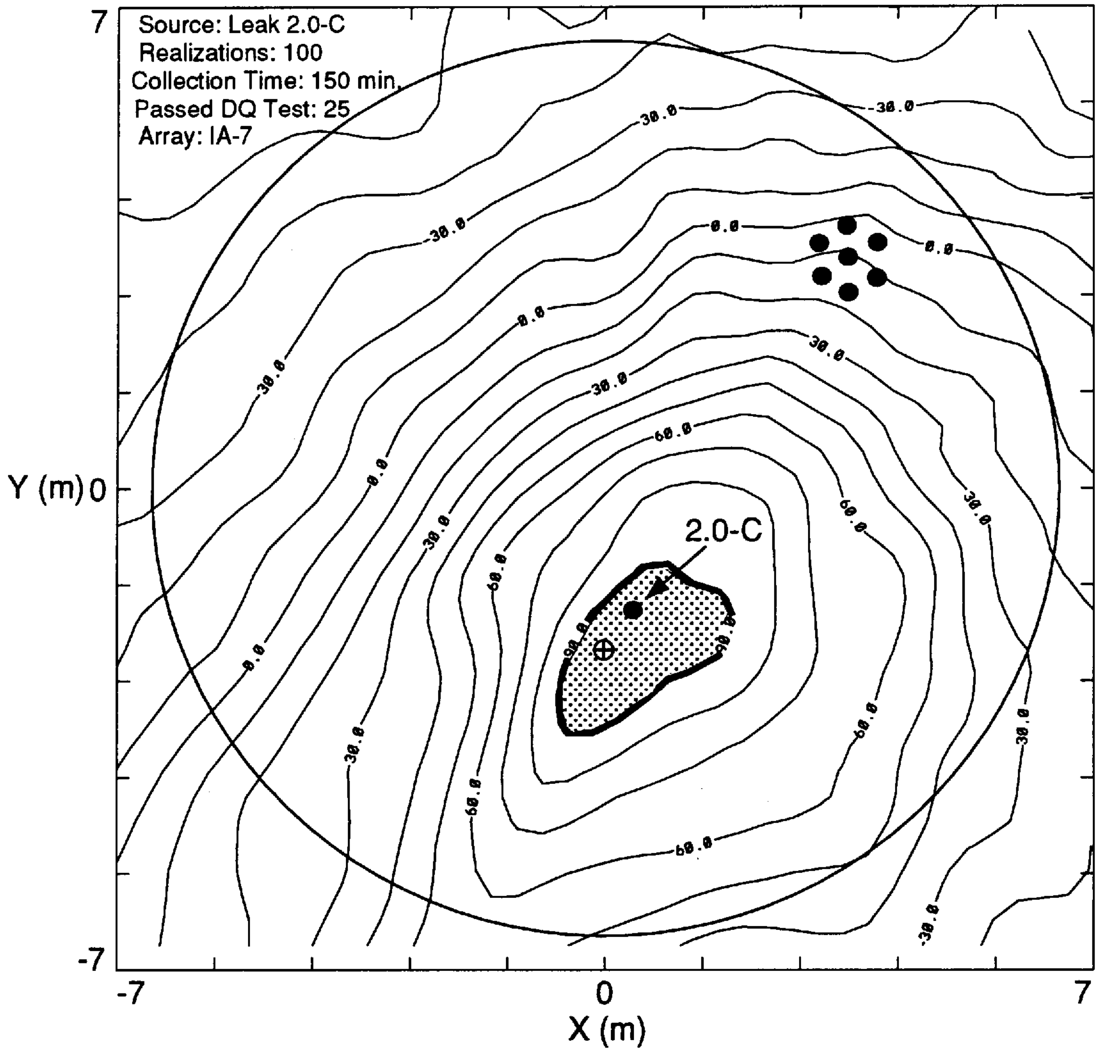

Figure 22. Map of SNR power as a function of position on the AST floor. Modified beamforming algorithm was applied to 100 realizations of the 2.0-C acoustic leak signal. Bold contour encloses region for which received SNR power is within 10% of the maximum. Maximum power location is indicated by marker. Secondary threshold is set to exclude multi-path signals.

important results. An acoustic leak detection system combining high-threshold acquisition of impulsive leak signals, collection of continuous time series, and data quality tests to reduce contamination by multi-path propagation was used to detect realistic leaks into two types of backfill and also to detect leaks generated by a leak simulator. While the impulsive component of the acoustic leak signal was successfully exploited for the purpose of leak detection, attempts to detect and locate AST leaks based on the persistent leak signal were unsuccessful.

The double-threshold approach to data collection and analysis outlined in this work serves as a means to avoid two problems associated with AST leak detection: noise-induced false alarms and multi-path signals caused by reflections within the AST interior. In order to minimize the probability that a given data set is contaminated by noise, the trigger threshold used to initiate data acquisition must be set far above the rms noise level. The primary threshold used to initiate data collection is influenced by noise fluctuations that occur on a time scale equal to the test duration (hours). Since the number of threshold exceedances caused by noise fluctuations is proportional to the threshold level *and* the time during which the threshold is in effect, a low-level primary threshold will present many data sets to the detection algorithm that are contaminated by noise. When a high threshold is used to initiate data collection, the quantity of data processed by the location algorithm is diminished, but the probability that a given data set contains information about a unique, locatable event is increased. Experimental data and ray-tracing simulations have shown, however, that data collected at *any* threshold level will be subject to some degree of contamination by multi-path signals. In order to identify data sets in which the trigger event corresponds to multi-path propagation, a secondary, low-level threshold must be applied to continuous time series of the leak signal. Since the secondary threshold is applied to time series of short duration (10 ms), noise fluctuations that can be misinterpreted as leak signals are statistically less likely. Application of the secondary threshold allows the arrival time of the direct-path impulse to be measured, even though the data collection was triggered by a multi-path signal. It should be noted that the identification and analysis of multi-path impulses provide an independent measure of the leak and its location.

RECOMMENDATIONS

Several additional experiments should be conducted in order to evaluate system performance and to demonstrate the robustness of passive-acoustic systems for the detection of leaks in ASTs. The program should be conducted in a manner that addresses the system performance in terms of the probability of detection and probability of false alarm as a function of leak size, AST geometry, product type, and ambient noise conditions.

The impulsive leak signal generated by the leak simulator was observed to be similar in character to the signals produced by realistic leaks (Appendix A). If controlled studies of the impulsive leak signal (laboratory simulations and test-tank experiments) show that this signal is indeed associated with a large class of AST leaks, then leak simulators should be installed in ASTs of larger diameter that contain a variety of products. Experiments with large tanks and different products are necessary to investigate the multi-path propagation effects over large distances, and to further develop the detection algorithm.

ACKNOWLEDGEMENTS

The authors gratefully acknowledge the cooperation of Mobil Oil Company, and in particular John Collins of the Beaumont Refinery, for providing the AST and the operational support necessary for the successful completion of the experimental portion of this work. We also wish to thank CTI, Inc., for providing the acoustic transducers and preamplifiers used in the experiment. This work was funded by a contract with the American Petroleum Institute. The authors would like to acknowledge the encouragement and technical review provided by the API Task Force monitoring this work.

REFERENCES

Carter, G. C. 1987. Coherence and Time Delay Estimation. *Proceedings of the IEEE*. 75:2.

Eckert, E. G., and J. W. Maresca, Jr. 1991. Detection of Leaks in the Floor of Aboveground Storage Tanks by Means of a Passive Acoustic Sensing System. *Air and Waste Management Association*. 91.15.5.

Miller, R. K. 1990. Tank Bottom Leak Detection in Above Ground Storage Tanks by Using Acoustic Emission. *Materials Evaluation*. 48(6):822-829.

Nickolaus, C. M. 1988. Acoustic Emission Monitoring of Aboveground Storage Tanks. *Materials Evaluation*. 46:508-512.

Smith, J. O., and Abel, J. S. 1987. Closed-Form Least-Squares Source Location Estimation from Range-Difference Measurements. *IEEE Transactions on Acoustics, Speech, and Signal Processing*. ASSP-35(12).

Van Veen, B. D., and Buckley, K. M. 1988. Beamforming: A Versatile Approach to Spatial Filtering. *IEEE ASSP Magazine*. 4:4-24.

Order No. 849-32200

80PP 02943C1P

RELATED API PUBLICATIONS...

PUBL. 323 January 1994	*An Engineering Evaluation of Volumetric Methods of Leak Detection Methods in Aboveground Storage Tanks*

To order, call API Publications Department (202) 682-8375

American Petroleum Institute
1220 L Street, Northwest
Washington, D.C. 20005